Pathways to sustainability or collapse in inland small-scale aquaculture systems: insights from a social–ecological systems model

Ecological Modelling 512 (2026) 111416

Contents lists available at ScienceDirect

Ecological Modelling

journal homepage: www.elsevier.com/locate/ecolmodel

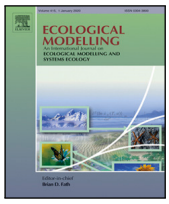

Pathways to sustainability or collapse in inland small-scale aquaculture systems: insights from a social–ecological systems model

Sonja Radosavljevic [a,*], Francesca Acotto [b], Quanli Wang [c], Jie Su [d,c], Alexandros Gasparatos [c]

[a] Department of Energy and Technology, Swedish University of Agricultural Sciences, 750 07 Uppsala, Sweden
[b] Dipartimento di Matematica"Giuseppe Peano", Università di Torino, via Carlo Alberto 10, 10123 Torino, Italy
[c] Institute for Future Initiatives, University of Tokyo, 7-3-1 Hongo, Bunkyo-ku, Tokyo 113-0033, Japan
[d] Fujian Provincial Key Laboratory for Coastal Ecology and Environmental Studies, College of the Environment and Ecology, Xiamen University, Xiamen, China

ARTICLE INFO

Keywords:
Bifurcation
Bistability
Dynamical system
Social–ecological system
Pond aquaculture
Sustainable intensification

ABSTRACT

Despite the promise of inland small-scale aquaculture for improving food security and alleviating poverty, the long-term sustainability of such production systems remains poorly understood, particularly in contexts where economic and ecological processes reinforce each other. This paper develops a stylized social–ecological model that captures feedbacks between producer wealth, fish biomass, and nutrient dynamics in inland pond-based small-scale aquaculture systems. The model reveals how these intertwined feedbacks shape the long-term dynamics of the system and lead to monostability, bistability, or multistability. These regimes correspond to a collapse, a high-yield but high-risk, and a sustainable equilibrium in fish production. Using bifurcation and stability analysis, we identify six dynamic scenarios: Balanced efficiency, Overload, Flux, Knife-edge, Tipping pond and Decay, that represent qualitatively different long-term outcomes. Rather than predicting specific outcomes, the model gives a structural understanding of small-scale aquaculture system dynamics and highlights the importance of local context and producers' heterogeneity in shaping the outcomes. It also provides a theoretical foundation for scenario-based management and empirical model development.

1. Introduction

Aquaculture has been one of the fastest-growing food production sector in the world, providing more than half of all fish for human consumption (FAO, 2020). At the same time, aquaculture development has been linked to several sustainability challenges, including social issues such as inequality and common-pool resource dilemmas, and ecological issues such as eutrophication and disease outbreaks (Nagel et al., 2024). There is also an ongoing debate on who and how much benefits from participation in aquaculture, with research supporting the view that it is beneficial primarily to those who can afford it (Belton, 2013), but also to the poorest of the poor (Pant et al., 2014).

An increasing fraction of aquacultural output comes from inland small-scale aquaculture (SSA) producers (FAO, 2020; Filipski and Belton, 2018). Many of them live in regions characterized by high poverty rates, few off-farm income and employment opportunities, and high vulnerability to market disruptions (Boughton et al., 2021; Kang et al., 2021). They are often exposed to financial, climatic, and environmental risks and frequently face food insecurity, social, and regulatory issues (Mitra et al., 2019; Rahman et al., 2021). Sometimes SSA producers have limited knowledge of the ecology of aquaculture ponds, which consist of many interdependent physical, chemical, and biological processes under anthropogenic and environmental influence (Boyd et al., 1998). Moreover, SSA producers generally lack access to improved farm technologies and production practices. As a result, many SSA production systems are not improved, preventing the producers achieving high productivity and income and essentially escaping poverty.

The central concern in this context is whether SSA production systems can avoid low-yield, low-investment traps and transition toward sustainable high-yield, high-income states. Unlike agriculture research, where these questions received considerable attention (Barrett and Carter, 2013; Lade et al., 2017; Radosavljevic et al., 2020, 2021; Sanga et al., 2024), aquaculture research rarely adopts a social–ecological system approach (Levin et al., 2013) to explore development pathways from a long-term dynamics point of view (Béné et al., 2016; Partelow et al., 2018). Most of the work is focused on conventional commercial monoculture systems, with very few exceptions that focus on small-scale aquaculture producers (Little et al., 2018; Naylor et al., 2023).

* Corresponding author.
E-mail address: sonja.radosavljevic@slu.se (S. Radosavljevic).

https://doi.org/10.1016/j.ecolmodel.2025.111416
Received 25 July 2025; Received in revised form 5 November 2025; Accepted 11 November 2025
Available online 21 November 2025

Furthermore, the broader inland aquaculture research has historically focused heavily on technical aspects of production and quantitative and qualitative impact assessment (Gephart et al., 2021; Henriksson et al., 2021; Naylor et al., 2021). Mathematical and simulation models applied in aquaculture research usually study biophysical dynamics and explore biotic and abiotic factors that affect fish growth and the behavior of ecological populations. These include the dynamic energy budget model (Kooijman, 2010), the thermal growth coefficient model (Jobling, 2003), the biomass-based models (Svirezhev et al., 1984), or individual-based models (Lu, 2003). In other cases, aquaculture models focus on bioeconomic dynamics (Nobre et al., 2009), optimization problems (Kvamsdal et al., 2020), or the effects of climate change (Varga et al., 2020). An exception is the work of Filipski and Belton (2018), which uses the general equilibrium model to study the effects of small-scale commercial aquaculture on poverty.

In general, little is known about how intertwined social and ecological processes shape the long-term dynamics of inland small-scale aquaculture systems and create structural low-yield traps. Few models include endogenous economic and ecological dynamics capable of generating multistability, bifurcation-induced tipping, or hysteresis. To address this gap, we develop a stylized dynamical model to explore how intertwined economic and ecological feedbacks shape the long-term dynamics of inland small-scale aquaculture systems.

The model draws on concepts from social–ecological systems research (SES) (Levin et al., 2013) and the dynamical system modeling applied to SES (Radosavljevic et al., 2023). Our aim is not to develop a predictive model that accurately represents the day-to-day operations of an inland SSA production system, nor to calibrate it to a specific empirical case study, but rather to explore the qualitative behavior and structural conditions under which such systems may experience different long-term outcomes. In this sense, the model functions as a theoretical tool for identifying possible dynamical regimes, such as system collapse, poverty traps, and risky high-yield attractors, and for clarifying how endogenous economic and ecological dynamics shape those outcomes. The model also explores the leverage points within the system where interventions could be useful and identifies critical points where shocks could be dangerous. Interventions in the context of the paper mean intentional exogenous short-term influence on the system, for example, short-term inputs of assets, nutrients, or training provided by institutions or Non-Governmental Organizations.

Unlike classic models where effort or capital investment is exogenous, our formulation allows wealth to evolve endogenously based on past production outcomes. Allowing wealth to evolve endogenously captures the feedback between production outcomes and future investment capacity, a mechanism central to poverty-trap dynamics in small-scale production systems. A poverty trap refers to an unwanted state of a system formed by self-reinforcing mechanisms that keep individuals in low-income and low-yield equilibrium (Barrett and Carter, 2013; Barrett et al., 2016; Haider et al., 2018). In multidimensional models with economic, cultural and ecological variables, it is possible to explore feedback-mediated traps, where productivity may fail to escape low-income, low-yield equilibria if reinvestment is limited, the environment is degraded, or cross-level interactions between individual producers and the community propagate the trap (Alkire et al., 2015; Lade et al., 2017; Haider et al., 2018).

To address these challenges, we develop a dynamical model to explore how inland small-scale aquaculture systems behave under such feedbacks. The purpose of the paper is two-fold. First, we aim to explore the long-term dynamics of inland small-scale pond aquaculture systems created by intertwined social–ecological processes. Second, we aim to identify leverage points within the system where interventions could be useful and to pinpoint critical points where shocks could have destabilizing effects.

The paper is organized as follows. In Section 2 we present the model of an inland pond-based small-scale aquaculture system, including its empirical and theoretical assumptions. Section 3 contains the main analytical results related to the model equilibrium points and the conditions for their feasibility and stability. Further mathematical details can be found in the Appendix. Section 4 explores long-term outcomes, attractors, and system resilience using stability analysis. We develop six dynamic scenarios to illustrate these findings. Section 5 explores bifurcations in detail, including pathways to transformation toward sustainable small-scale aquaculture systems. Section 6 discusses implications for research and management.

2. Stylized model of an inland pond-based small-scale aquaculture system

This section has two objectives. First, we describe the conceptual model that underlies the mathematical model. Second, we develop the mathematical model using a system of nonlinear ordinary differential equations.

2.1. Conceptual model

We base our causal understanding of the inland pond-based small-scale aquaculture system on empirical studies such as Belton (2013), De Silva and Davy (2010), Filipski and Belton (2018) and Fish for Livelihoods (2022), and the first-hand experience of three of the authors conducting small-scale aquaculture research in developing countries such as Myanmar, Egypt, and Bangladesh (Dam Lam et al., 2022; Dompreh et al., 2024; Rossignoli et al., 2023a,b; Wang et al., 2023, 2024). In short, small-scale aquaculture is an activity that produces fish in inland water bodies (e.g. rivers, lakes) for household consumption and sales in the market. In this sense, it can contribute to household nutrition and income generation, having a positive outcome for food security and livelihood.

Small-scale producers are generally poor and face food insecurity. Adopting fish culture or increasing the technical efficiency of existing fish production can increase levels of income and fish consumption, and consequently reduce producers' poverty and food insecurity. Achieving high yields and product quality in aquaculture systems requires maintaining adequate water quality and nutrient supply. However, pond ecosystems are characterized by complex interactions between physical, chemical, and biological processes (Boyd et al., 1998). These dynamics are further shaped by environmental variability and human management, often at multiple spatial and temporal levels.

Although tools from system ecology can be very useful for modeling such complexity, representing every biophysical and socioeconomic detail is neither feasible nor necessary for our research aim. Instead, we develop a stylized conceptual model that focuses on key feedbacks driving the long-term dynamics of small-scale aquaculture systems. Our objective is to capture the qualitative behavior of the system and explore conditions under which multiple stable states, such as high-yield or low-yield equilibria, can coexist. The model is grounded in the following assumptions.

(1) Increased aquaculture production increases the income of small-scale aquaculture producers;
(2) Higher producer income enables greater investment in production inputs (e.g., improved feed, high-quality fingerlings), which in turn enhances fish growth;
(3) Increased fish growth has positive effects on fish biomass and production;
(4) Nutrient availability positively affects fish growth, but excessive nutrient loading can degrade water quality, ultimately reducing growth and increasing mortality.

These relationships form the basis for a conceptual model that represents key feedbacks in the inland pond-based small-scale aquaculture system. The conceptual model is illustrated in a causal loop diagram in Fig. 1. It captures the long-term dynamics shaped by interlinked

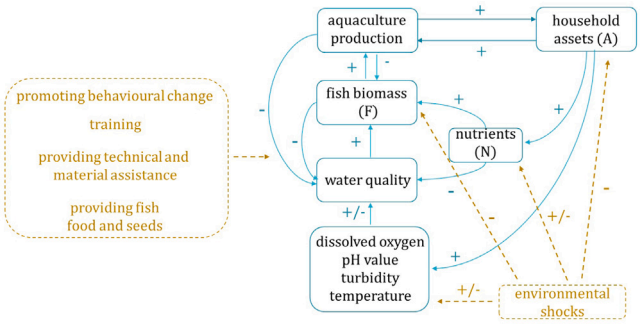

Fig. 1. Causal loop diagram for the stylized inland pond-based small-scale aquaculture system model. Blue arrows represent long-term processes in the system. External interventions and shocks are given in yellow. Dashed arrows represent short-term processes.

biochemical, economic, and social–ecological processes, including fish growth, nutrient input and cycling, and asset accumulation through production.

External interventions and shocks (e.g., climatic events, market shocks, financial disruptions) are modeled as perturbations to the system's states rather than changes in the system's structure. This allows us to investigate how the system's internal structure influence its trajectory under different starting conditions and short-term disruptions.

2.2. Baseline mathematical model

Based on the conceptual model and Fig. 1, we select the state variables for the mathematical model: household assets, A, fish biomass, F, and nutrients, N. The choice of assets and fish biomass reflects their central roles in both the economic viability and biological productivity of small-scale aquaculture systems. The choice of nutrients, rather than water quality, requires explanation.

Nutrient availability positively affects fish growth, but excessive nutrient loading can degrade water quality, ultimately reducing growth and increasing mortality. In the conceptual model (Fig. 1), we represent these effects as two distinct causal arrows: one capturing the positive role of nutrients for fish biomass growth, and another capturing the negative effects of excessive nutrients on mortality and ecological degradation. This separation is important to keep the conceptual assumptions transparent.

In translating the conceptual model into the mathematical model, we do not model these two arrows as separate state variables. Instead, a single nutrient variable N captures both effects. This is accomplished through functional forms that are positive at moderate levels and negative at high levels. The choice reflects a general principle in stylized modeling where conceptually distinct processes are not always represented as distinct state variables mathematically, if they can be captured by nonlinearities in a single variable.

Water quality is an inherently multidimensional property, encompassing diverse dimensions such as temperature, pH, dissolved oxygen, and turbidity, among others. Modeling each of these dimensions would require additional nonlinear dynamics, many of which are outside the direct influence of producers. Stylized models need clear boundaries, and here our aim is not to reproduce in detail every dimension of water quality, but to capture the minimal structure that generates the regimes of interest. Representing nutrients as a single state variable is sufficient to reproduce collapse, bistability, and oscillations, while keeping the model transparent and analytically tractable. More detailed formulations could add realism but would not necessarily add structural insight into poverty traps or sustainable intensification, which is the focus of this paper. Nonlinear formulations of nutrient loss (e.g., through sedimentation or chemical processes) could be possible extensions of our model, but the linear form used here is a common approximation in ecological models, as it enables model transparency while still capturing the essential feedbacks.

Nutrient dynamics are also more tractable and strongly influenced by human activities such as land use, feed type, and feed application rates. Modeling nutrient concentration as a state variable therefore enables capturing both the beneficial effects of moderate enrichment on fish growth and the detrimental effects of excessive nutrient loading, such as eutrophication or hypoxia. In this way, nutrients arguably serve as a proxy for water quality, enabling us to incorporate anthropogenic feedbacks and ecological processes within a simplified but ecologically meaningful model.

Assets dynamics. We extend the classical Solow model (Barro and Sala-i Martin, 2004), in which output depends on both assets (capital) and labor, by substituting labor with fish biomass. This formulation allows us to represent production in small-scale aquaculture systems, where fish biomass is the main biophysical driver of productivity. The production function is in Cobb–Douglas form:

$$f(A, F) = bA^{\alpha}F^{\beta},$$

where $b > 0$ denotes the productivity factor and reflects the knowledge, practices, and technology of SSA producers. According to Asamoah et al. (2012), small- and medium-scale aquaculture producers exhibit constant or increasing returns to scale, with elasticity coefficients $\alpha + \beta \geq 1$.

To capture empirically observed threshold effects in smallholder savings behavior, we follow Kraay and Raddatz (2007) and use an S-shaped savings rate $s(A) = s\frac{A^2}{p+A^2}$ that increases with assets. This formulation captures key nonlinearities in household decision-making, while maintaining consistency with empirical work such as Abdul Latif Jameel Poverty Action Lab (J-PAL) (2019) and Asamoah et al. (2012).

The rate of change of household assets is then modeled as:

$$\frac{dA}{dt} = bs\frac{A^2}{p+A^2}A^{\alpha}F^{\beta} - qA, \tag{1}$$

where the first term represents income reinvested into the system and the second term denotes depreciation or maintenance costs. As in the classical Solow model, we assume that asset depreciation is proportional to total assets. This assumption simplifies the analysis while maintaining consistency with standard macroeconomic and poverty trap models. It also reflects the idea that maintenance or capital loss is proportional to the assets total value. More complex asset outflows may be relevant but would require additional empirical validation and structural assumptions that are beyond the scope of this paper.

Fish dynamics. The classical bioeconomic model (Clark, 2010) assumes that the fish population growth follows the logistic equation

$$\frac{dF}{dt} = rF - mF - cF^2 - hF,$$

where the positive term rF denotes the fish biomass growth, and the negative terms $-mF$ and $-hF$ denote mortality and harvest proportional to the fish biomass, respectively. The negative term $-cF^2$ represents intraspecific competition for resources.

In small-scale aquaculture systems, harvesting is often periodic: farmers fill the pond, stock it with fingerlings, allow fish to grow, and then harvest them all at once before restarting the cycle. This means that harvest is not constant, but likely occurs in pulses. There are also cases in which the pond is continuously harvested and restocked. However, for simplicity, we model harvest as a constant rate proportional to fish biomass.

This simplification has three purposes. First, it allows us to work with an autonomous dynamical system, which is easier to analyze. Introducing a periodic harvest function would make the system non-autonomous and remove the possibility of classical attractors, making it necessary to study pullback attractors instead. Second, harvest can be interpreted as additional fish mortality that reflects not only actual harvest by the producer, but also predation, overcrowding effects, fish

Table 1
List of parameters used in model (4).

Parameters	Interpretation	Values	References
b	Factor of productivity	[0.1, 1.5]	Asamoah et al. (2012)
s	Assets savings rate	[0.1, 0.5]	Abdul Latif Jameel Poverty Action Lab (J-PAL) (2019)
p	Half-saturation point of assets savings rate	[5, 50]	Comparable with the value of assets at equilibrium
q	Assets depreciation rate	[0.05, 0.5]	Nobre et al. (2009)
α, β	Elasticity coefficients	$\alpha + \beta \geq 1$	Asamoah et al. (2012)
r	Fish growth factor	[0.002, 0.008]	Scheffer (1989)
u	Nutrient uptake rate	[0.1, 1]	Assumed within plausible biological range
v	Square of the optimal nutrient concentration	[1, 10]	Comparable with the value of nutrients at equilibrium
m	Fish mortality rate	[0.002, 0.01]	Scheffer (1989)
c	Fish competition rate	[0.001, 0.002]	Reflects pond size and fish density
h	Harvest rate, broadly defined as additional fish mortality	$h \geq 0$	Assumed to reflect management practices and external drivers
k	Agricultural run-off nutrient input rate	[0, 5]	Assumed due to large empirical variability
g	Fish feed nutrient input rate	[0.1, 1]	Assumed proportional to production effort
z	Half-saturation point of nutrient input rate	[1, 10]	Comparable with the value of nutrients at equilibrium
ℓ	Natural nutrient loss rate	[0.1, 1]	Assumed, reflects sedimentation and overflow

loss due to disease, poor water quality, high water temperature, or poor management practices. Third, since our goal is to understand long-term dynamics and qualitative system behavior, rather than accurately simulate short-term production cycles, the assumption of constant harvest captures the average effects over time and keeps the model easier to interpret.

Nutrients play a critical role in shaping fish growth dynamics, but the relationship between nutrient concentration and fish growth is not straightforward. At low to moderate levels, nutrients enhance fish growth as they support food availability. However, if nutrient levels become too high, water quality can deteriorate, which can reduce growth or even increase fish mortality. To capture both effects, we model the fish growth rate as a function of nutrients: $r(N) = ru\frac{N}{v+N^2}$. Thus, the classical logistic fish growth equation is modified as follows:

$$\frac{dF}{dt} = ru\frac{NF}{v+N^2} - mF - cF^2 - hF. \tag{2}$$

Nutrient dynamics. Nutrients enter the pond water from two main sources: constant agricultural run-off, denoted by k, or fish feed, expressed as $g\frac{AF}{z+A}$. The functional form implies that the nutrient input depends on the fish biomass and the producers assets. When asset levels are low, nutrient input is limited by the producer's capacity to purchase feed. At a high asset level, the nutrient amount is proportional to the fish biomass and limited by the amount of fish feed needed.

Nutrients are removed from the system in two ways. First, they are removed through uptake by the fish, which is expressed as $-u\frac{NF}{v+N^2}$ and represents an increasing function that saturates for high values of N. Second, nutrient loss due to natural processes, modeled by $-\ell N$, represents sedimentation, dilution, or effects of microbes. These considerations lead us to the following equation for the nutrient dynamics:

$$\frac{dN}{dt} = k + g\frac{AF}{z+A} - u\frac{NF}{v+N^2} - \ell N. \tag{3}$$

Combining Eqs. (1)–(3), we come to the model of SSA system:

$$\begin{aligned}
\frac{dA}{dt} &= bs\frac{A^2}{p+A^2}A^{\alpha}F^{\beta} - qA,\\
\frac{dF}{dt} &= ru\frac{NF}{v+N^2} - mF - cF^2 - hF,\\
\frac{dN}{dt} &= k + g\frac{AF}{z+A} - u\frac{NF}{v+N^2} - \ell N.
\end{aligned} \tag{4}$$

All model parameters, their meanings, or range of values, are specified in Table 1.

2.3. Price responsive variant

To connect the model more directly to market signals and producers' financial decisions while keeping it simple, we introduce a variant in which a few parameters respond to fish biomass and input prices, P_f and P_{in}, respectively. We retain the same state variables (A, F, N) and the same structure as in Eq. (4), but the productivity factor, nutrient intake rate and harvest rate are now functions of prices.

We define marketed biomass as

$$Q = h(P_f)\,F.$$

Fish price decreases with marketed biomass,

$$P_f = \frac{P_{f0}}{1+\beta_f Q}, \qquad \beta_f \geq 0,$$

and input price P_{in} is taken as given or scenario dependent. Prices are assumed to be in partial equilibrium. The three parameters that respond to prices have the following forms:

$$b(P_f, P_{in}) = b_0\left(\frac{P_f}{P_{in}}\right)^{\eta}, \qquad \eta > 0,$$

$$u(P_{in}) = u_0\left(\frac{P_{in0}}{P_{in}}\right)^{\mu}, \qquad \mu > 0,$$

$$h(P_f) = h_0\left(\frac{P_f}{P_{f0}}\right)^{\phi}, \qquad \phi > 0.$$

The form of the productivity parameter b captures stronger investment incentives when the fish price is high relative to the input price. The form of nutrient uptake rate u captures reduced effective feed use when inputs are expensive. The form of the variable harvest rate corresponds to a higher harvest rate when fish prices are high. Baseline prices P_{f0} and P_{in0} can be normalized to one so that h_0, u_0, and b_0 are baseline values.

Substituting these into Eq. (4) yields

$$\begin{aligned}
\frac{dA}{dt} &= b(P_f, P_{in})\,s(A)\,A^{\alpha}F^{\beta} - qA,\\
\frac{dF}{dt} &= r\,u(P_{in})\frac{NF}{v+N^2} - mF - cF^2 - h(P_f)F,\\
\frac{dN}{dt} &= k + g\frac{AF}{z+A} - u(P_{in})\frac{NF}{v+N^2} - \ell N.
\end{aligned} \tag{5}$$

All analytical and numerical results in the main text use the baseline system in Eq. (4). The price responsive variant is used to interpret how market signals and producers' decisions shift thresholds and basin sizes, without changing the qualitative results identified by the baseline model presented in the upcoming sections.

3. Long-term system outcomes and analytical insights

By developing a dynamical system model, we make use of two mathematical techniques: analysis of stability and bifurcations. Stability analysis studies the existence and properties of equilibrium points and explores the long-term dynamics of the system. Bifurcation analysis investigates how changes in parameter values lead to qualitatively different behavior of the model.

In practical terms, stable equilibria represent development pathways, such as persistent poverty (system collapse), production associated with risks, or sustainable aquaculture. This section presents the mathematical foundation for these regimes by identifying feasible equilibrium states and their stability. These results enable us to locate thresholds and tipping points in the system and assess how investment, nutrient levels, climatic shocks, or other short-term events might move the system from one state to another. Although the analysis is technical, it provides essential groundwork for the numerical analysis in Section 4 and the policy-relevant insights discussed afterwards. Readers who are not interested in the mathematical analysis of the model can safely skip this section, continuing to Section 4. Those interested in more mathematical details can find them in the Appendix.

The model (4) is nonlinear and fairly difficult to explore analytically. To enable some of the analytical methods for stability investigation, we simplify the model by assuming the maximal assets savings rate and the elasticity coefficients equal to one, i.e., $s = \alpha = \beta = 1$. With this assumption, the model reads as follows:

$$\begin{aligned}\frac{dA}{dt} &= b\frac{A^2}{p+A^2}AF - qA,\\ \frac{dF}{dt} &= ru\frac{NF}{v+N^2} - mF - cF^2 - hF,\\ \frac{dN}{dt} &= k + g\frac{AF}{z+A} - u\frac{NF}{v+N^2} - \ell N.\end{aligned} \tag{6}$$

The following two subsections are devoted to the analytical study of this simplified model, in particular, its equilibrium points' feasibility and local stability. The main results are summarized in Table 2. Additional mathematical insights are given in the Appendix.

3.1. Feasibility of equilibrium points

The simplified model (6) allows only the following three equilibria:

$$E_C = \left(0, 0, \frac{k}{\ell}\right), \quad E_P = \left(0, F_P, N_P\right), \quad E_* = (A_*, F_*, N_*).$$

The equilibrium with only nutrients, or the collapse equilibrium, E_C, is explicitly known and unconditionally feasible. Instead, the nonlinear system (6) is too complex to explicitly determine the components of the equilibrium without assets, i.e., the poverty trap, E_P, and those of the coexistence equilibrium, E_*. However, we can look for sufficient conditions for their feasibility.

In the assets-free case, we can look for conditions that ensure at least one graphical intersection point, in the first quadrant of the N-F plane, between two curves we find from the equilibrium equations. In the coexistence case, similarly, we are interested in intersecting three surfaces in the first octant of the A-N-F space. The sufficient conditions for the feasibility of E_P and E_* given in Table 2 are obtained in the Appendix.

3.2. Local stability of equilibrium points

The Jacobian of the model (6) is

$$J = \begin{bmatrix} J_{11} & \frac{bA^3}{p+A^2} & 0\\ 0 & \frac{ruN}{v+N^2} - (m+h) - 2cF & ruF\frac{v-N^2}{(v+N^2)^2}\\ gF\frac{z}{(z+A)^2} & \frac{gA}{z+A} - \frac{uN}{v+N^2} & J_{33}\end{bmatrix}, \tag{7}$$

where

$$J_{11} = bF\frac{3A^2(p+A^2) - 2A^4}{(p+A^2)^2} - q, \quad J_{33} = -uF\frac{v-N^2}{(v+N^2)^2} - \ell.$$

3.2.1. Nutrients-only point, E_C

By evaluating (7) at equilibrium E_C, a lower triangular matrix is obtained, from which the eigenvalues are easily found. They are

$$-q, \quad -f, \quad \frac{ruk\ell}{v\ell^2 + k^2} - (m+h).$$

Thus, we have the following local asymptotic stability condition:

$$ruk\ell < (m+h)(v\ell^2 + k^2). \tag{8}$$

3.2.2. Assets-free point, E_P

At E_P the characteristic equation factorizes and one eigenvalue is explicitly found, that is, $-q$. This eigenvalue is always negative, thus it does not affect the local asymptotic stability of the assets-free equilibrium point.

We use the notation $J_{[m,n]}$ for the submatrix of J in which the rows and columns m and n are preserved. For the remaining 2×2 minor, $J_{[2,3]}(E_P)$, we use the Routh–Hurwitz criterion. The determinant of this minor is

$$\det(J_{[2,3]}(E_P)) = cF_P\left[\ell + uF_P\frac{v-N_P^2}{(v+N_P^2)^2}\right] + ruF_P\frac{v-N_P^2}{(v+N_P^2)^2}\frac{uN_P}{v+N_P^2}.$$

Its trace, instead, using the second equilibrium equation, reduces to

$$\mathrm{tr}(J_{[2,3]}(E_P)) = -cF_P - \ell - uF_P\frac{v-N_P^2}{(v+N_P^2)^2} < 0.$$

Thus, the Routh–Hurwitz condition on the determinant gives the following local asymptotic stability condition:

$$\begin{aligned}cF_P\left[\ell + \frac{uvF_P}{(v+N_P^2)^2}\right] + \frac{ruvF_P}{(v+N_P^2)^2}\frac{uN_P}{v+N_P^2} &> \frac{ruF_PN_P^2}{(v+N_P^2)^2}\frac{uN_P}{v+N_P^2}\\ &+ \frac{cuF_P^2N_P^2}{(v+N_P^2)^2}.\end{aligned} \tag{9}$$

3.2.3. Coexistence, E_*

In the coexistence case, we can find the local asymptotic stability condition using the Routh–Hurwitz criterion for a cubic equation, i.e., $RH3(J(E_*))$. However, an explicit determination of $RH3(J(E_*))$ is too much involved and will not shed more light on the problem, so we do not analytically investigate them further. We explore the coexistence point stability using numerical methods in the following section.

4. Scenarios as different futures

Modeling nonlinear systems is rarely a linear process. During this process, we alternate between stability analysis that is used to explore the behavior of the system for fixed parameter values and bifurcation analysis, which reveals how qualitative dynamics changes when parameters change. Stability analysis offers a snapshot of possible outcomes under a fixed combination of parameters, while bifurcation analysis helps us explore how these outcomes evolve across different ecological or economic contexts. To organize insights of the stability analysis, we develop a set of scenarios that represent distinct long-term regimes. These scenarios capture combinations of attractors and they are presented in this section. Section 5 then examines the bifurcations in more detail and traces the pathways that lead systems toward sustainability or collapse as underlying conditions change. Since our observations and results have to be presented in a linear way in the paper, we ask readers for patience as some results may be fully understood once both this and Section 5 are read.

The purpose of this section is to use stability analysis to explore the long-term dynamics of the model. The analysis in Section 3 shows that the model (6) can have one or more stable equilibrium points (attractors) depending on the parameter values. We use numerical methods to identify the attractors and analyze the implications of their location in phase space (Figs. 2 and 3). Table 3 contains standard values of the parameters used in the models.

Table 2
Equilibria of model (6): feasibility and local stability conditions. If there is more than one point E_*, we assign them labels E_S and E_R to indicate sustainable and risky states. More details can be found in Section 4 and Table 4.

Equilibria	Feasibility	Local stability
$E_C = \left(0, 0, \frac{k}{\ell}\right)$	Unconditionally feasible	Asymptotically stable iff (8)
$E_P = (0, F_P, N_P)$	Not feasible if (12), with (13) or (15), when (16)	Asymptotically stable iff (9)
	Feasible and unique if (12), with (13) or (15), when (17)	
	Saddle–node if (12), with (13) or (15), when (18) and (19)	
$E_* = (A_*, F_*, N_*)$	See Tables 6, 7, 8, 9, 10, and 11	Asymptotically stable iff $RH3(J(E_*))$

Table 3
Standard values of parameters of model (4).

Parameters	b	s	p	q	α	β	r	u	v	m	c	h	k	g	z	ℓ
Standard values	1	0.3	10	0.4	0.5	0.5	0.9	0.3	2	0.009	0.001	0.001	0.1	0.1	5	0.1

Table 4
Equilibria of model (6): interpretation of their properties in real systems.

Attractor name	Mathematical label	Interpretation
Collapse	$E_C = \left(0, 0, \frac{k}{\ell}\right)$	Economically and ecologically degraded state; highly resilient to shocks
Poverty trap	$E_P = (0, F_P, N_P)$	Unbalanced input use; no assets due to low returns; highly resilient to shocks
Sustainability state	$E_S = (A_S, F_S, N_S)$	Productive and ecologically balanced state; fairly resilient to shocks
Risky state	$E_R = (A_R, F_R, N_R)$	Highly productive and ecologically balanced state; very vulnerable to shocks

Attractors located closer to the origin represent less desirable system states. The reason is simple: points close to the origin are characterized by low values of assets, fish biomass, and nutrients. Low assets and fish biomass indicate poverty and low productivity. While low to medium nutrients indicate an ecologically balanced state, high nutrients, especially if fish biomass is low, may indicate an ecologically degraded state.

We interpret resilience as the system's vulnerability to shocks and potential for regime shifts. To assess resilience, we estimate the distance between the attractor and the edge of its basin of attraction (separatrix). Attractors closer to the separatrix are considered more vulnerable to shocks. To make these implications more accessible, we assign intuitive labels to the attractors: collapse, poverty trap, risky state, and sustainability state. Table 4 provides a detailed characterization of these states.

We explore six scenarios that correspond to different combinations of parameter values. Each scenario represents qualitatively different long-term outcomes depending on the number and type of attractors. In some cases, the system has two attractors: the poverty trap and the sustainability state. In other cases, a third attractor or a stable limit cycle appears. It is also possible for the system to have a single attractor, but it is always only the undesirable one, collapse, or poverty trap. A sustainability attractor never appears on its own, but always coexists with at least one undesirable alternative.

The scenarios were identified through bifurcation analysis. We examined patterns in the number and stability of attractors, the width of parameter intervals, and the relative size of basins of attraction to distinguish qualitatively different dynamical regimes. These mathematical regimes were then linked to real-world interpretations, for example, a knife-edge scenario reflecting high sensitivity to shocks.

Rather than offering precise predictions of what will happen, these scenarios are stylized representations of how the system could behave under plausible variations in key drivers. Their purpose is to guide thinking about the long-term dynamics of the system, management options, risks, and leverage points. The scenarios are summarized in Table 5.

4.1. Balanced efficiency

This scenario reflects situations when good economic conditions (e.g. medium productivity and reinvestment efficiency), meet favorable ecological conditions (e.g. low nutrient runoff and loading), and good management practices that enable fish survival even in heavy-stocked ponds. Bistability emerges, and it is represented by the poverty trap and the sustainability state (Fig. 2A).

Due to the low external nutrient loading, most nutrients enter the system through fish feed. This gives producers the opportunity to actively manage the dynamics of the pond. It also makes nutrients a more controllable part of the system. As a result, nutrient levels play a relatively minor role in shaping the basins of attraction. Their shape is captured in Fig. 2A. If both assets and fish biomass are sufficiently high, the system moves toward the sustainaility attractor, E_S. If not, the trajectories converge toward the poverty trap E_P.

In this scenario, both the poverty trap E_P, and the sustainable equilibrium, E_S, are insensitive to changes in nutrient levels. Even large fluctuations in nutrients levels are unlikely to have lasting effects on the system's behavior. In contrast to this, changes in fish biomass or assets can lead not only to temporary effects, but also to regime shifts. The sustainability state may be lost after shocks that significantly reduce fish biomass or assets. Similarly, targeted interventions that increase assets and fish biomass can tip the system from poverty toward recovery and long-term sustainability.

4.2. Overload

This scenario depicts situations where high productivity and low return on investment are combined with high agricultural nutrient loading. Bistability and the chance of sustainable production arise but are strongly dependent on controlling nutrient inputs.

Fig. 3 highlights the importance of nutrients in shaping the basins of attraction and illustrates the complex interactions between the state variables. Panel A shows Tipping pond scenario, i.e., a multistable system with low agricultural nutrient runoff. The risky state exists

Table 5
Possible long-term scenarios depending on ecological and economic conditions.

Scenario	System properties	Conditions	Implications
Balanced efficiency	Bistable system with Poverty trap and Sustainability state	High productivity, reinvestment efficient even at low asset levels, low nutrient run-off (low k, high c, low p) (Fig. 2A)	Well managed system; insensitive to nutrient fluctuations; changes in fish biomass and/or assets can tip the system
Overload	Bistable system with Poverty trap and Sustainability state	High productivity, reinvestment efficient only at high asset levels, high nutrient run-off (high k, low c, high p) (Fig. 3B)	Bistability enabled by low intraspecific competition; sustainability possible only at low nutrient levels; sensitivity to changes in all variables, especially nutrients
Flux	Bistable system with Poverty trap and stable limit cycle	Average productivity, reinvestment efficient even at low asset levels, low nutrient run-off and intraspecific competition (low k, low c, low p) (Fig. 5)	The system oscillates due to interactions between ecological and economic processes. Collapse can be avoided, but managing such system can be challenging because periods of high assets and fish biomass are followed by periods of low assets and fish biomass.
Knife-edge	Bistable system with Poverty trap and Risky state	Below average productivity, reinvestment efficient even at low asset levels, low nutrient run-off and intraspecific competition, fish is well-adapted to low nutrient conditions (low k, low c, low p) (Figs. 4, 5, 6)	Very sensitive to financial shocks, efficient feeding practices keep nutrient level low. The scenario often exists only for a very narrow parameter range.
	Multistable system with Poverty trap, Risky and Sustainable attractors	Sensitivity of this scenario comes from a very limited parameter range for which it exists. The system is more resilient to changes in its states than to changes in the ecological or economic conditions. (Fig. 7)	The combination of sensitivity to parameters, initial conditions and shocks makes desired outcomes difficult to achieve and keep.
Tipping pond	Multistable system with Poverty trap, Sustainability state and Risky state	Above average productivity, reinvestment efficient even at low asset levels, low nutrient run-off and intraspecific competition (low k, low c, low p) (Figs. 3A, 4, 5)	Risky state is desirable due to high asset accumulation and high fish biomass, but it is difficult to preserve. Collapse is avoided due to existence of a resilient sustainability state that offers modest, but stable returns.
Decay	Monostable system with Collapse or Poverty trap	Extreme conditions (e.g. very low or very high productivity or input rate) provide temporary boost, but long-term collapse (Figs. 4, 5, 6, 7, 8)	Economically and/or ecologically degraded system; system recovery would require a system transformation to create a sustainability attractor

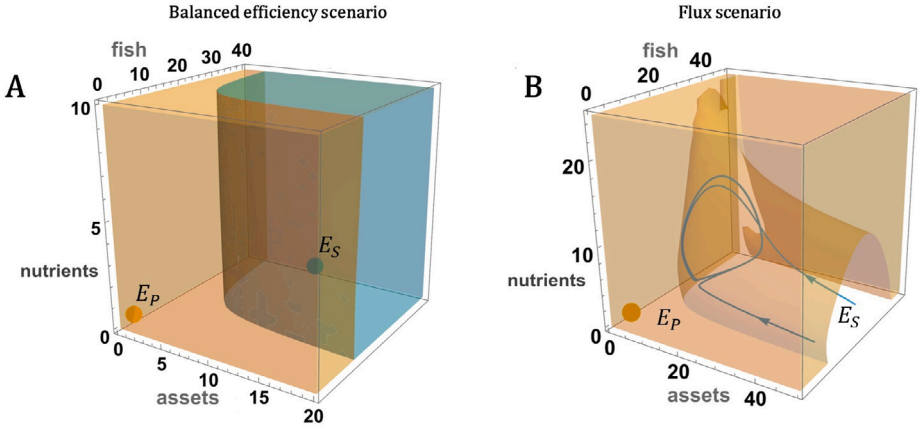

Fig. 2. The model (4) is bistable for various combinations of the parameter values. The standard values are indicated in Table 3. (A) Balanced efficiency scenario with $v = 5$, $c = 0.002$. (B) Flux scenario with $p = 50$, $k = 0.5$. Poverty trap attractor, E_P, is the undesired low-yield equilibrium and sustainability attractor. Yellow volume is the basin of attraction of the poverty trap. Rest of the phase space are states that converge toward the limit cycle. Blue lines are two such trajectories.

and is reachable for a specific combination of assets, fish biomass and nutrients. Increasing agricultural runoff leads to a qualitative change in the dynamics of the system and the emergence of an Overload scenario. Here, the Risky state E_R disappears and the Sustainability state E_S becomes less resilient. Reaching E_S requires initial conditions with sufficient assets, fish biomass, and low nutrient levels. If any of these conditions is not met, the system shifts toward the poverty state, E_P.

Compared to the Balanced efficiency scenario, the Overload scenario reveals how higher runoff nutrient input and a larger half-saturation constant for savings amplify the role of nutrients. The resilience of the sustainable attractor is reduced, while the poverty trap becomes more robust. Overcoming it may require a simultaneous reduction in nutrient levels and an increase in both assets and fish biomass.

4.3. Flux

Flux refers to a scenario in which the system exhibits bistability between a stable limit cycle and a poverty trap (Fig. 5). This dynamic arises within a relatively narrow range of savings rates ($s \in (0.25, 0.3)$), where ecological and economic feedbacks interact to produce sustained oscillations in assets, fish biomass, and nutrients. These oscillations reflect stability in a mathematical sense, but may be challenging in real world systems. Outcomes are not fixed but fluctuate, which may offer a periodic surplus in fish biomass and income, but also risks (e.g., periodic crashes or exposure to shocks at low points in the cycle).

In a narrow subinterval of the savings rate, the system briefly exhibits three coexisting attractors: the poverty trap, the sustainable

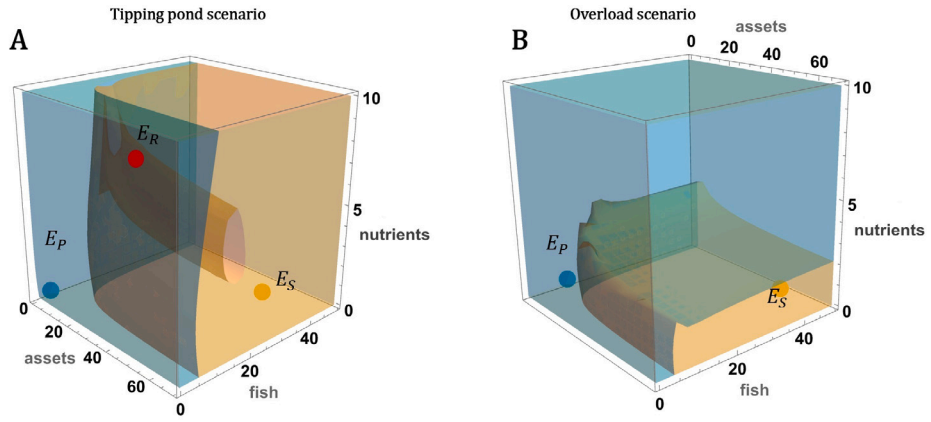

Fig. 3. (A) Tipping pond scenario ($b = 1.67$, $p = 50$). (B) Overload scenario ($b = 1.6$, $p = 50$). Poverty trap attractor, E_P, is the undesired low-yield equilibrium and Sustainability attractor, E_S, is the high-yield equilibrium. E_R is the risky state that appears for low nutrient runoff. Colored volumes represent basins of attraction of the three attractors.

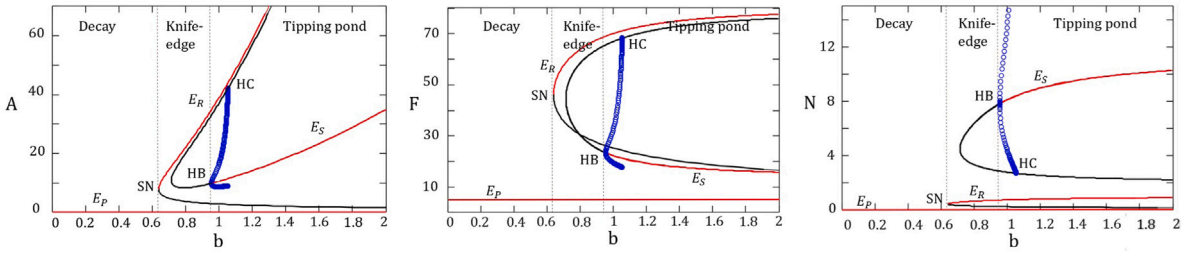

Fig. 4. Bifurcation analysis shows the existence of one, two, or three stable equilibrium points for different values of the parameter b. Red lines denote stable equilibrium points. Black lines denote unstable equilibria. Blue circles are unstable limit cycles. E_P is the branch of Poverty trap attractors. E_R and E_S are branches of Risky and Sustainability attractors. Saddle–node, Hopf, and homoclinic bifurcations are denoted by SN, HB, and HC, respectively. Dashed lines indicate parameter thresholds that separate scenarios (see Table 5 for details). The parameter values are in Table 3. Reading b as $b = b_0 (P_f/P_{in})^{\eta}$ implies a price-ratio threshold $(P_f/P_{in})_{\text{crit}} = (b^*/b_0)^{1/\eta}$ at point SN.

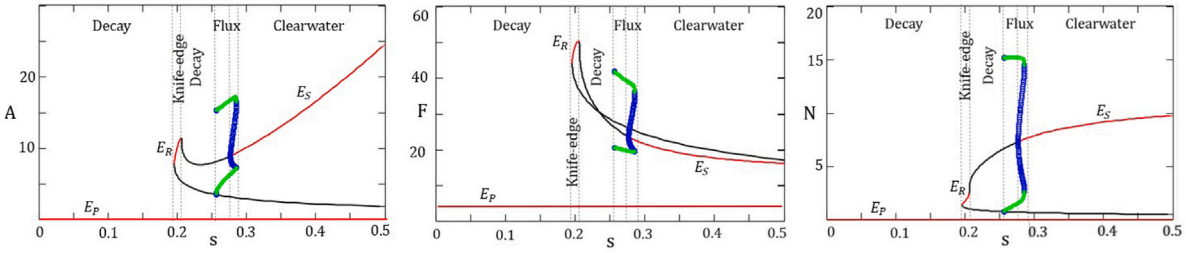

Fig. 5. Bifurcation analysis for different values of the parameter s. The parameter values are $v = 0.5$ and the others are indicated in Table 3. Red lines denote stable equilibrium points. Black lines denote unstable equilibria. Blue circles are unstable limit cycles. Green circles are stable limit cycles. E_P is the branch of Poverty trap attractors. E_R and E_S are branches of Risky and Sustainability attractors. Dashed lines indicate parameter thresholds that separate scenarios (see Table 5 for details).

state, and the limit cycle. This window is small but structurally meaningful. It shows that efficient returns on investment in combination with low nutrient run-off and low intraspecific competition may create a balanced trajectory that stabilizes oscillations and prevents fall into poverty. The presence of stable limit cycles suggests that timing, shock sensitivity, and the adaptive capacity of producers play crucial roles in determining outcomes.

4.4. Knife-edge

Knife-edge describes a scenario where desirable outcomes exist but are difficult to reach and even harder to maintain. It has two variants. The first is a bistable system with a poverty trap and a risky state (Figs. 4–6). This state emerges around average productivity, efficient reinvestment (even at low asset levels), and low levels of nutrient run-off and intraspecific competition. The second variant is a multistable system with a poverty trap, a risky state, and a sustainability attractor (Fig. 7). This variant appears when additional mortality is nearly zero or harvest is extremely controlled. In other words, it requires a fine-tuned parameter setting.

This scenario exists for either a very narrow parameter range, or the desired attractor is very close to the separatrix, which makes it fragile. In either case, the geometry of the system often makes the desirable attractor difficult to maintain due to high sensitivity to initial conditions and perturbations.

Knife-edge scenario appears often in our analysis, indicating rich but fragile dynamics of small-scale aquaculture ponds. If the system could remain in the risky state, Knife-edge would be one of the most desirable

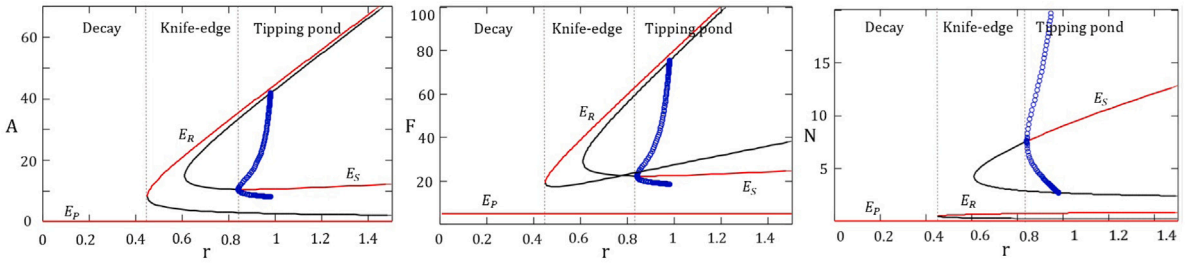

Fig. 6. Bifurcation analysis for different values of the parameter r. Other parameter values are indicated in Table 3. Red lines denote stable equilibrium points. Black lines denote unstable equilibria. Blue circles are unstable limit cycles. E_P is the branch of Poverty trap attractors. E_R and E_S are branches of Risky and Sustainability attractors. Dashed lines indicate parameter thresholds that separate scenarios (see Table 5 for details).

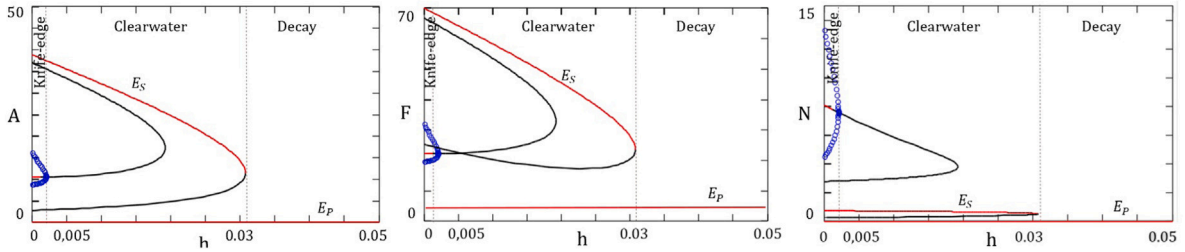

Fig. 7. Bifurcation analysis for different values of the parameter h with $m = 0.01$. Other parameter values are indicated in Table 3. Red lines denote stable equilibrium points. Black lines denote unstable equilibria. Blue circles are unstable limit cycles. E_P is the branch of Poverty trap attractors. E_S are branches of Risky and Sustainability attractors. Dashed lines indicate parameter thresholds that separate scenarios (see Table 5 for details).

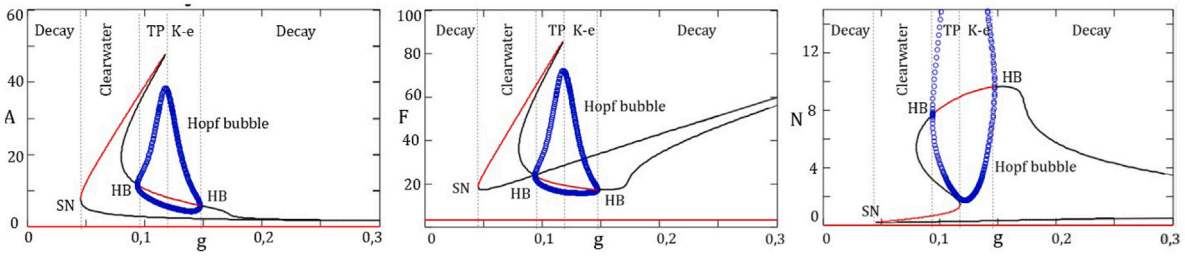

Fig. 8. Bifurcation analysis shows the existence of one, two, or three stable equilibrium points for different values of the parameter g. Other parameter values are indicated in Table 3. Saddle–node and Hopf bifurcations are denoted by SN and HB, respectively.

outcomes, offering high asset accumulation and fish biomass with low to moderate ecological degradation.

4.5. Tipping pond

Tipping pond represents a scenario with three stable states, one of which has a narrow basin of attraction and can easily tip due to a shock. It often emerges for a high saving rate or a high fish growth rate (Figs. 5 and 6).

Fig. 3A suggests that the basin of attraction of the poverty trap (blue volume containing E_P) comprises initial states with a low level of assets or a low level of fish biomass. The basin of attraction of E_S comprises initial states with sufficiently high values of fish biomass and assets. The most unusual and potentially counterintuitive basin of attraction is the one containing the risky state E_R (volume containing the red dot). It is characterized by initial conditions with intermediate nutrient values, a narrow range of intermediate fish biomass, and all, except very low levels of assets.

The trajectories converging towards E_R can be disturbed by increasing nutrient levels, which would force them toward E_S. Another possibility is drastically reducing the level of assets or fish biomass and forcing trajectories toward E_P. Risks in the system can come in different forms, but do not have to lead to catastrophic outcomes. Using the same reasoning, we can assess the efficiency of management strategies and interventions. To be efficient, a poverty alleviation strategy should increase the assets or fish biomass and probably reduce the nutrients in the system.

4.6. Decay

There are two variants of the Decay scenario. One in which Decay represents an economically dysfunctional, but ecologically viable system with Poverty trap as a single attractor. The other alternative is a system that is both economically and ecologically degraded and where Collapse is the single attractor.

There are many pathways to the Decay scenario. Some of them involve decreasing income and/or fish biomass due to low productivity or input rates, while others emerge through nutrient input, eutrophication, or worsening economic conditions leading to a low return on investment (high values of the parameter p).

The global stability of the attractor in this scenario makes it particularly resilient to any kind of short-term intervention, regardless of its intensity or where in the system they are applied. Short-term improvements in productivity or ecological conditions are likely to occur, but achieving permanent changes in the way the system behaves requires a transformation of the system. By transformation we mean

changing the strength of feedbacks that created the trap and enabling the emergence of the Sustainability attractor.

5. Bifurcations and shifting scenarios

Stability analysis provides information about the system for fixed values of its parameters. However, parameters can change over time or across geographical locations, and it is important to understand how such changes affect the system's long-term behavior. In structurally unstable systems, the dynamics can change qualitatively when parameters pass threshold values. These thresholds, known as bifurcation points, can mark transitions between desirable and undesirable system states. Knowing the properties of system dynamics under different parameter settings or uncertainty improves understanding of the system and supports better management decisions. Therefore, we use bifurcation analysis to explore qualitative changes in system structure and to identify leverage points and potential risks across a plausible range of parameter values.

The derivation in Section 3 showed that the analytical results are hard to obtain even for the simplified model (6). The parameters α and β were eliminated in the simplified model (6) by setting them to 1. However, they are very important for understanding the consequences of social–ecological interactions related to the use of new technology. Changes in the values of these parameters can be understood as the adoption of innovation and training. The parameters b, p, and q are related to productivity, assets saving, and depreciation rate, respectively. Together, they determine whether aquaculture becomes a reinforcing loop of growth or stagnates due to low returns or high losses.

Similarly, the parameters k and g define the amount of nutrients that enter the system, unintentionally as runoff (in the case of k) or intentionally through fish feed (in the case of g). These parameters can be related to producers' decisions, their capacity to manage agricultural and aquacultural nutrients and to choose the type and amount of fish feed.

The parameters r, u, and v describe ecological processes of growth and nutrient uptake and depend on species, local ecological conditions, and the type of fish feed. These parameters influence how responsive the system is to nutrient input and how easily growth becomes limited or destabilized.

5.1. Productivity

The bifurcation diagram in Fig. 4 shows changes in the number and stability of the equilibrium points when the parameter b is varied. The poverty trap, E_P, exists for all parameter values, reminding us that system collapse is always an option. Increasing the productivity parameter, b, creates the second stable equilibrium point, E_R, through a saddle–node bifurcation. Increasing b even more leads to a Hopf bifurcation and the appearance of the third stable equilibrium point, E_S.

These transitions illustrate how the dynamics of the system changes through three scenarios. For low values of b, the system is in the Decay scenario (Table 5) where only the poverty trap exists (Fig. 4). Recovery is not possible within the current structure.

As the parameter b increases, the system enters the Knife-edge scenario, where the poverty trap and the risky state coexist. The resilience of E_R is low, especially with respect to changes in assets. It is a desirable state but difficult to maintain, giving the name of the attractor. The system is very sensitive to initial conditions and shocks, especially those that decrease assets or productivity, but there is a chance to avoid collapse.

A further increase in productivity leads to the emergence of the sustainability state, marking the Tipping Pond scenario, where three attractors coexist. Maintaining high productivity and biomass is tricky because the risky attractor, E_R, is highly sensitive to shocks and initial conditions. The sustainability attractor, E_S, prevents slipping into economic and ecological degradation and offers a reliable pathway.

Using price responsive model (5) allows us to read movements along the b axis as movements in an effective productivity factor $b = b_0 (P_f/P_{in})^{\eta}$. A threshold value b^*, for which the saddle–node bifurcation in the diagram appears, therefore corresponds to a critical price ratio $(P_f/P_{in})_{\text{crit}} = (b^*/b_0)^{1/\eta}$. Price ratios above this level increase effective productivity and allow the existence of E_R and E_S, while lower ratios lead to permanent poverty.

5.2. Savings rate

The bifurcation diagram in Fig. 5 shows how the long-term behavior of the system changes when the savings rate, s, is varied. This parameter plays a central role in asset dynamics, shaping the capacity of small-scale aquaculture producers to accumulate and reinvest.

In our model, we explore the interval of plausible savings rate. For $s < 0.18$, the system collapses into the Decay scenario, where only the poverty trap exists and recovery is impossible without transformation of the system. At $s \approx 0.18$ a new stable state emerges, leading to the Knife-edge scenario, where recovery is possible but fragile and highly dependent on initial conditions.

However, this opportunity is short-lived. As s increases, the system returns to the Decay scenario. This is an unexpected result given the common assumption that higher savings always improve outcomes. This suggests that saving without sufficient productivity or ecological resilience can backfire, for example by reducing short-term liquidity or delaying investment in fish feed or water infrastructure.

Beyond $s \approx 0.25$, the system shifts into the Flux scenario, where stable oscillations co-exist alongside the poverty trap. Here, the long-term pattern has inherent variability and risk. Finally, at $s \approx 0.31$, the system enters the Balanced efficiency scenario, with a stable and resilient sustainability attractor.

This complex pattern implies that modest savings rates, consistent with empirical observations, do not guarantee stability or success. Instead, outcomes depend on where in the interval the system lies and whether other conditions (e.g., productivity, nutrient loading) support reinvestment effectiveness. The policy implication is clear: encouraging savings is not enough unless the broader ecological and economic structure enables those savings to translate into productive improvements.

5.3. Fish growth rate

The fish growth rate plays a central role in shaping the long-term behavior of the small-scale aquaculture system. The bifurcation diagram in Fig. 6 illustrates how changes in parameter r affect the number and type of attractors in the system.

For low values of r, the system exhibits a monostability characterized by the poverty trap, E_P. This is a Decay scenario in which fish do not grow fast enough to support production or investment, leading the system to collapse over time, regardless of initial conditions.

As the fish growth rate increases to intermediate values, a new stable equilibrium, E_R, emerges through a saddle–node bifurcation. This bistability defines the Knife-edge scenario, where the system can either fall back into the poverty trap or climb toward a more productive regime, depending on the initial levels of fish biomass, nutrients, and assets. However, the risky attractor is located close to the separatrix, which makes it vulnerable to fluctuations in all three state variables, especially in decrease in fish biomass and assets and an increase in nutrients.

At high values of r, a third attractor emerges through a Hopf bifurcation. The system now exhibits Tipping Pond dynamics with three coexisting attractors. This multistability increases the complexity of management because the risky state, E_R, becomes even more fragile, while the sustainability state, E_S, becomes more resilient. Transitions between high-yield, high-income regime and sustainable regime may occur due to very small changes in any of the variables.

This progression of scenarios, from collapse, to conditional recovery, to full multistability, highlights how increase in fish growth (e.g., through better species selection, higher quality fingerlings, better feed, or pond management) can open up new possibilities but also increase the chance of mismanagement.

Since fish biomass growth is tightly connected with quality and quantity of inputs, and they depend on price and producers' financial decisions, we use price sensitive model (5) to explore these effects. We map the growth term ru to an effective coefficient $r_{\text{eff}} = r\,(u(P_{in})/u_0) = r\,(P_{in0}/P_{in})^{\mu}$. Hence a saddle–node bifurcation at $r = r^*$ corresponds to a critical input price $P_{in}^{\text{crit}} = P_{in0}(r/r^*)^{1/\mu}$. If the inputs are cheaper than the critical value, $r_{\text{eff}} > r^*$ and bistability is possible. If the inputs are more expensive, the system falls in the Decay scenario.

5.4. Harvest and additional fish mortality

The bifurcation diagram with respect to the harvest rate h shows a sequence of qualitative transitions in the system dynamics (Fig. 7). For very low harvest rates, the system exhibits the Knife-edge scenario, where multistability emerges between the poverty trap, a sustainable and a risky, high-yield state. The very narrow range of h makes this scenario difficult to maintain.

As h increases, the Knife-edge scenario shifts into the Clearwater scenario, where sustainable production is possible, but sensitive to shocks. Further increases in h lead to a Decay scenario, where all attractors disappear through a saddle–node bifurcation, except for the poverty trap.

The parameter h represents continuous harvest, but is also a proxy for additional fish mortality caused by predation, overcrowding, poor water quality, disease, or high water temperature. Throughout the whole parameter range, the levels of assets, fish biomass, and nutrients steadily decline as the parameter h increases. These results suggest that even seemingly insignificant additional mortality can destabilize long-term productivity.

To link market conditions and producers' decisions to shifts between scenarios as observed in the baseline model we use price sensitive harvest rate. In the price responsive variant we write $h(P_f) = h_0\left(P_f/P_{f0}\right)^{\phi}$ with $\phi > 0$, so movements along the h axis can be read as movements in the fish price. A threshold value h^* in the diagram therefore corresponds to a critical price

$$P_f^{\text{crit}} = P_{f0}\left(\frac{h^*}{h_0}\right)^{1/\phi}.$$

Prices above P_f^{crit} imply higher harvest intensity and that can push the system toward the regions with Balanced efficiency or Decay outcomes, while prices below P_f^{crit} are consistent with the low-harvest side where Knife-edge multistability occurs.

5.5. Feed input

The parameter g represents the contribution of fish feed to nutrient input. The bifurcation analysis reveals a non-monotonic relationship between nutrient input and the system's long-term behavior (Fig. 8).

For low values of g, nutrient levels are insufficient to support fish growth, leading the system to collapse or decay. As nutrient levels increases to low-intermediate values, the system enters a Clearwater scenario characterized by bistability between collapse and desirable state.

A further increase in nutrient input leads to a Tipping Pond scenario through a Hopf bifurcation. The newly emerging attractor is encircled by unstable limit cycles within a Hopf bubble. However, this regime only appears in a narrow window of above-average nutrient input, suggesting that it is difficult to achieve or maintain in practice.

As g continues to increase, the system shifts into a bistable regime again, but one where the sustainability state requires high initial values of assets and fish biomass, but does not preserve these high levels for long. For most other initial conditions, the system converges to collapse. Finally, for very high nutrient input, the system collapses again, likely due to ecological degradation and feedbacks that reduce fish survival despite having sufficient nutrients.

This complex progression from poverty trap to eventual escape from poverty and back to it suggests that nutrient input is a double-edged sword. Both too little and too many nutrients can drive the system toward undesirable outcomes and Decay scenarios. Only an intermediate range of nutrient input supports stable and desirable aquaculture dynamics.

The central part of the bifurcation diagram shows behavior that resembles hysteresis. Typical hysteresis in ecological models is represented by two saddle–node bifurcations that have a common branch of unstable equilibrium points, Scheffer (1989). Behavior in this model is richer and more nuanced because two Hopf bifurcations create a Hopf bubble of unstable limit cycles. The stable branch within the bubble can only be reached by trajectories that originate within the bubble, with others being repelled toward alternative attractors.

6. Discussion

6.1. Structural understanding

The model developed in this paper is based on social–ecological systems research (Levin et al., 2013) and has a strong focus on poverty traps (Barrett and Carter, 2013; Barrett et al., 2016; Haider et al., 2018). Previous models of poverty traps have been used as exploratory tools to provide insight into the dynamics of a system, test hypotheses, develop scenarios and answer the "what if" questions (Banitz et al., 2022; Eppinga et al., 2024). The models were mainly conceptual, rooted in the neoclassical economic tradition (Barro and Sala-i Martin, 2004), and discussed economic causes and solutions to poverty (Barrett et al., 2016; Blume et al., 2020). In recent years, multidimensional poverty trap models of agricultural systems have been introduced. The authors focused on small-scale subsistence agriculture and investigated the role of nature and culture in alleviating poverty (Lade et al., 2017), the role of assets, water, and nutrients (Radosavljevic et al., 2020), the impact of cross-level interactions between individual and community levels (Radosavljevic et al., 2021), the emergence of cross-level poverty traps in agricultural innovation systems (Sanga et al., 2024), or the impact of disease and poor health on persistent poverty (Ngonghala et al., 2014, 2017).

Most of the poverty trap models are formalized as systems of ordinary differential equations and represent intertwined social–ecological processes observed in real systems. The model in this paper is based on the same principles and is analyzed using the same mathematical methods. The causal structure of the model is based on stylized facts from the published literature and first-hand the experience of the coauthors to specifically represent the small-scale aquaculture system. Combined analytical and numerical techniques allow for the study of the long-term dynamics of a small-scale aquaculture system in a fairly transparent way.

The number and type of equilibrium points, the size and shape of basins of attraction, bifurcations, and tipping points can be clearly identified, giving a qualitative understanding of the system. However, the clarity these models provide rests on simplification and abstraction. Regime shifts, resilience of poverty traps, vulnerability to shocks, or other dynamic patterns described in the model may therefore bear little relation to the real system. Dynamical system modeling is best used jointly with empirical research and more complex modeling approaches, in an iterative process where assumptions and results can be tested and validated (Eppinga et al., 2024; Radosavljevic et al., 2024; Sanga et al., 2024).

In this sense, the objective of dynamical systems models—including our model—is not to predict or prescribe, but to provide structural

understanding: revealing how system structure generates behavior (Radosavljevic et al., 2023). Social–ecological dynamics and possible causal relationships are revealed through the manipulation of interactions between state variables and the observation of their consequences (Schlüter et al., 2024). Structural understanding is particularly valuable for assessing the effectiveness of interventions, the consequences of shocks, and managing transformation toward sustainable outcomes.

Our contribution should also be understood in the context of a much broader body of work on modeling social–ecological systems. As highlighted by Bialozyt et al. (2025), and Nugroho (2025), a central challenge is to operationalize SES models in ways that balance empirical detail, disciplinary perspectives, and system complexity. Many SES models emphasize either conceptual richness or detailed case-specific calibration, often at the cost of analytical tractability.

In contrast, our model is deliberately positioned as a stylized dynamical systems model which has two key advantages. First, it makes the underlying causal structure transparent and allows the conditions for multistability and collapse to be mathematically identified. Second, it enables generalization beyond individual case studies by revealing structural mechanisms, such as savings-mediated poverty traps or nutrient-driven collapse, that appear in aquaculture settings. Our work fits within the theory-oriented category of SES models described by Jakeman et al. (2024), which prioritize structural understanding over case-specific prediction or decision support. By formulating a low-dimensional dynamical system, we make feedbacks and thresholds analytically tractable, complementing more empirically detailed approaches. This aligns with Section 4 of Jakeman et al. (2024), where stylized models are highlighted as essential for identifying general mechanisms that can guide data collection and applied modeling efforts.

Rather than competing with more data-driven approaches, our model provides a theoretical lens that helps identify where empirical models should look for thresholds, trade-offs, and leverage points. More broadly, the same principles apply to other small-scale production systems, such as agriculture, forestry, or common-pool fisheries, where economic–ecological feedbacks shape long-term sustainability.

6.2. Implications for sustainable intensification

Transforming aquaculture in developing countries from extensive to intensive is done with the clear aim of improving livelihoods and food security. However, it entails a set of challenges that are neither fully understood nor easy to assess. The challenges are connected to tension between sustainability and productivity and solving them requires a clearer understanding of how intertwined ecological, technological, economic, and social processes shape dynamics in multidimensional settings. In agricultural poverty alleviation, for example, there is a tendency to use blanket solutions without paying enough attention to the local context and the social–ecological complexities of the system (Barrett and Carter, 2013; Haider et al., 2018). The consequences of such practices can be dire and even reinforce the dynamics they were set to break (Lade et al., 2017).

Here, we investigate how two dimensions of social–ecological complexity, the local context and the producer heterogeneity, enable, prevent, or shape achieving sustainable outcomes in small-scale aquaculture.

6.2.1. Local context

The local context in the paper represents a combination of parameter values that describe specific social–ecological conditions in the model and lead to certain long-term dynamics. We identified six scenarios, i.e., qualitatively different long-term dynamics, which we labeled Clearwater, Overload, Knife edge, Flux, Tipping pond, and Decay (Table 5). These scenarios can be used as depictions of alternative futures in real systems.

The bifurcation analysis in Section 5 shows that the qualitative behavior of the model (4) is rich and highly context-dependent. Changing the context can cause the system to shift from one scenario to another and, in doing so, open or close a pathway to sustainable production and ecosystem management. With price-responsive parameters, movements in productivity translate market conditions and producers' decisions into shifts of thresholds and basin sizes, which helps explain why similar interventions succeed in one context and fail in another.

Among the scenarios we identified, Balanced efficiency and Tipping Pond look like the most promising long-term alternatives for sustainable outcomes. They are characterized by desirable attractors with relatively high fish biomass and asset levels and a large basin of attraction. In the case of Tipping Pond, there is often a less desirable alternative attractor that offers higher assets and fish biomass, but a very small basin of attraction. In other words, Tipping Pond can be structurally fragile and highly sensitive to fluctuations, but it does not easily flip to a degraded state.

Knife-edge and Flux scenarios are less favorable. In Knife-edge scenario, the desirable attractor is difficult to reach and easy to lose due to a very narrow parameter range for which the scenario exists. Small shocks or suboptimal starting conditions can quickly lead to collapse. Flux scenario describes systems with stable limit cycles, where outcomes heavily oscillate due to interactions between ecological and economic feedbacks. Sustainability of outcomes is not reliable as it depends on timing and strength of perturbations, changes in the local context and producers heterogeneity. Finally, the Decay scenario represents system failure where collapse occurs regardless of initial conditions. This scenario is always associated with low productivity, with or without ecological degradation, and the absence of recovery pathways.

This progression from collapse to fragile sustainability and back to collapse illustrates that interventions must be tailored not only with expected outcomes in mind, but also to fit the underlying scenario. Without accounting for this complexity, best wishes may lead to suboptimal results or failure.

6.2.2. Producer heterogeneity

Producer heterogeneity is expressed by differences in assets, fish biomass, and nutrient levels. In the model, each producer is identified with a unique set of initial conditions (i.e., a triplet (A_0, F_0, N_0)) located in the phase space. These differences reflect the variation in wealth, fish availability, and pond properties, and they strongly shape effects of local context and outcomes of interventions.

The model shows that small differences in initial conditions can result in very different long-term outcomes. Placing initial conditions in different basins of attraction means that their trajectories will converge toward different outcomes. Stability analysis in Figs. 2 and 3 reveals who is more resilient or more at risk, or who in a heterogeneous group of producers would benefit from an intervention and who would be left behind. Price-responsive parameters help interpret which producers are most exposed. For example, households with low initial assets, A_0, or a high harvest rate, h_0, are more likely to cross price thresholds where the price sensitive harvest $h(P_f)$ increases, or the price sensitive nutrient uptake, $u(P_{in})$, decreases, moving them into less favorable basins.

The poverty trap in Decay scenarios can be alleviated only by a series of interventions, where the first needs to transform the system and create an alternative sustainable or risky attractor. Subsequent interventions can then focus on adjusting initial conditions and moving them into the newly created basin of attraction.

In bistable and three-stable systems, it is possible to escape ecological degradation and poverty without transforming the system. Interventions must place the system in the desired basins of attraction. Figs. 2 and 3 show which state variables should be targeted to achieve this. In Fig. 2A, an intervention should aim to increase assets and/or fish biomass, while in Fig. 3B, it should also decrease nutrients.

The analysis reveals that the shape and size of basins of attraction depends on the local context. Fig. 2A describes the scenario in which it is easier to reach a higher savings rate and the input of runoff nutrients is lower compared to the scenario in Fig. 3B. The same initial conditions that would lead to well-being in the first scenario could lead to the poverty trap in the second scenario. This sensitivity highlights the importance of understanding both the number and nature of attractors and basins of attraction, and using that knowledge to design interventions that are context-dependent and tailored to specific producer conditions.

6.3. Links to case studies and implications for management

Several recent empirical studies have examined the sustainability outcomes of interventions in small-scale aquaculture, highlighting their potential to improve food availability (Wang et al., 2024) and enhance livelihoods (Dam Lam et al., 2022), although it is not always clear through which pathways diversification stabilizes food security and livelihoods. The literature also suggests that the impact of such interventions on poverty remains ambiguous. Belton and Little (2011) claim that: "As total volume and value of output are likely to correspond closely to the area of pond under culture, even where poorer producers can be engaged the absolute benefits they derive are likely to be smaller than those of better-off project participants with larger land-holdings". Cramb et al. (2004) supports these findings and states that the impact of small-scale aquaculture is likely to be highly class-differentiated. This result is well supported by our findings. As Figs. 4–8 show, producers who initially have more assets, higher fish biomass, and better ecological conditions are more likely to reach risky and sustainable attractors and escape persistent poverty. The same intervention can therefore be more beneficial for producers who are better off from the beginning.

The interventions described by Wang et al. (2024) increase productivity, probably by increasing productivity and feed input, that is, by increasing values of parameters b and g. This creates bistable systems, as shown in Figs. 4 and 8. Dam Lam et al. (2022) examines an ecopond model in Bangladesh that aims to increase diverse food consumption and women empowerment. The project focused on women training (increasing parameter b) and utilizing ecosystem services (keeping k and g low). The results show how intensification can lead to improved sustainability, but not across all dimensions or for all producers. This resembles the Balanced efficiency and Tipping pond scenarios in Fig. 8, where producers' heterogeneity and vulnerability to shocks play an important role in determining the outcome of an intervention. Unlike the original study, our model does not assess cultural and socioeconomic barriers to women empowerment or equity.

The bifurcation diagrams in Figs. 4 and 8 can also be used to explore the results of Belton and Little (2011) and Cramb et al. (2004). According to the model, intensification can create a suboptimal attractor in a three-stable system. The consequence of intensification is that its positive effects could be unevenly distributed among poor and wealthy producers. Wealthy producers are in a better position to benefit from interventions because they are more likely to be in the sustainable or risky basin of attraction, while poor producers have a higher chance of being caught in the undesired state near the poverty trap.

Our results suggest that similar outcomes can emerge through different mechanisms, reflecting the diversity of pathways observed in empirical studies. A deeper understanding of particular cases could take the modeling further, for example, by highlighting the key structural elements that should be included in the model, adjusting parameter ranges, and offering a more nuanced view of the research questions and interpretation of results.

Close collaboration between modelers, practitioners, and stakeholders is essential to ensure that models remain empirically grounded and useful in real world contexts. Stability and bifurcation analyses could then serve as tools to navigate the complexity of specific cases, to support the design of interventions and to help anticipate their potential unintended effects.

6.4. Implications for research

There are many ways in which the model presented in this paper can be expanded to explore relevant research questions. We list several of them that align with our research interests and open research questions, but the list is in no way complete.

The dynamics of small-scale aquaculture ponds is affected by temperature variation and is strongly dependent on the biophysical properties of the pond (Bieg and Vasseur, 2024; Jobling, 2003; Lu, 2003). Including spatio-temporal variability in models would increase their mathematical complexity because it requires nonautonomous systems of ordinary or partial differential equations. However, it would allow us to explore the interplay between spatio-temporal patterns with social–ecological processes in the system. Including more details on the ecological side could help explore polyculture ponds (Milstein, 1992) and the effects of disease spread on poverty (Hoover et al., 2019).

The problems in governing small-scale aquaculture systems can be seen as social dilemmas in which shared water or space are examples of common pool resources (Partelow et al., 2022). Demographic heterogeneity, that is, differences in producers' wealth, training, opinions, and perceived risks, could be reflected in their preferred strategies and decisions and play an important role in shaping the small-scale aquaculture dynamics (Rahman et al., 2021; Nagel et al., 2024). The effects of social norms and management strategies on producers' decisions, and in turn on small-scale aquaculture dynamics, can be explored using combinations of dynamical systems, evolutionary game-theoretic, and agent-based models.

There is a lack of firm knowledge on financial, climatic, and environmental shocks and their effects on aquaculture dynamics (Luna et al., 2023). Dynamical systems typically focus on asymptotic behavior and processes that last forever, but including transient analysis can give answers to questions concerning shorter time periods and instantaneous processes. These results could contribute to understanding out-of-equilibrium dynamics and inform stakeholders and management about efficient ways to adapt and respond to shocks.

Another important area for future work is the explicit treatment of uncertainty. Considering the general lack of dynamic models for small-scale aquaculture systems, our model should be seen as a first effort to reveal which dynamic behaviors are possible. However, it does not quantify how plausible these behaviors are under current knowledge through an explicit quantitative uncertainty analysis. Uncertainty quantification through sensitivity analysis or probabilistic parameter ranges would move the analysis closer to answering how near real systems might be to tipping points and which data gaps matter most. Although such methods go beyond the scope of this paper, we must point out that this is a critical direction for future research.

A further promising direction is the integration of price dynamics and market feedbacks into SSA models. Economic incentives influence harvest timing, input use, and investment decisions and can amplify shocks or enable recovery. Including price dynamics explicitly using additional state variables for market dynamics could reveal new pathways of collapse and recovery that are not captured by the model presented here. This is particularly relevant for small-scale producers, whose decisions are often shaped by short-term price fluctuations. Simple price-responsive formulations, as in our price-responsive model, can help translate bifurcation thresholds into critical price ratios, but more elaborate endogenous price models could explore how coupled ecological–economic instabilities emerge through feedback loops between production and markets.

CRediT authorship contribution statement

Sonja Radosavljevic: Writing – review & editing, Writing – original draft, Visualization, Software, Methodology, Investigation, Funding acquisition, Formal analysis, Conceptualization. **Francesca Acotto:** Writing – original draft, Funding acquisition, Formal analysis. **Quanli**

Wang: Writing – original draft, Funding acquisition, Conceptualization. **Jie Su:** Writing – original draft, Funding acquisition, Conceptualization. **Alexandros Gasparatos:** Writing – original draft, Funding acquisition, Conceptualization.

Declaration of competing interest

The authors declare that they have no known competing financial interests or personal relationships that could have appeared to influence the work reported in this article.

Acknowledgments

The authors wish to express their sincere gratitude to Professor Ezio Venturino for his generous guidance and substantial intellectual contributions to the development of this work. His insights and enthusiasm for mathematical modelling greatly enriched this study, and we are grateful for the time and care he shared with us.

SR has been supported by the Swedish Research Council FORMAS (grant number 2021-01840). AG, QW, and JS acknowledge technical support funding provided by WorldFish as part of the project "Characteristics and impacts of aquatic food systems". FA has been partially supported by the project "Analisi di metodi ed algoritmi in teoria dell'approssimazione e modelli in biologia ed ecologia" (Analysis of methods and algorithms in approximation theory and models in biology and ecology) of the Dipartimento di Matematica "Giuseppe Peano" of the University of Torino.

Appendix

In this appendix, we provide mathematical details related to the feasibility of the assets-free equilibrium, E_P, and coexistence, E_*, summarized in Table 2 of Section 3.

Feasibility of assets-free point, E_P

From the second equilibrium equation of the model (6), i.e., equilibrium equation for F, we obtain $F = \Psi(N)$, where

$$\Psi(N) = \frac{ruN}{c(v+N^2)} - \frac{m+h}{c}. \tag{10}$$

On the other hand, from the third equilibrium equation, i.e., equilibrium equation for N, we explicitly get $F = \Theta(N)$, where

$$\Theta(N) = \frac{v+N^2}{uN}(k - \ell N).$$

Thus, for the feasibility of E_P we can look for sufficient conditions to have at least one intersection point between the curves Ψ and Θ in the first quadrant of the N-F plane.

Study of the curve Ψ

The function $\Psi(N)$ for $N \geq 0$ is a gamma-like function. Its intersection with the vertical axis and its horizontal asymptote are, respectively, given by $\left(0, -\frac{m+h}{c}\right)$ and $F_a = -\frac{m+h}{c}$. Therefore, it lies outside the feasible region unless its peak, located at $N = N_*$, has a positive height, $\Psi(N_*) > 0$.

The maximum can easily be established by differentiation, giving

$$N_* = \sqrt{v} \quad \text{and} \quad \Psi(N_*) = \frac{ru\sqrt{v}}{2cv} - \frac{m+h}{c}, \tag{11}$$

and the feasibility condition

$$ru > 2(m+h)\sqrt{v}. \tag{12}$$

Then, the function $\Psi(N)$ intersects the horizontal axis whenever

$$(v+N^2)(m+h) - ruN = 0.$$

The latter is a quadratic equation, whose roots are explicitly found:

$$N_\pm = \frac{1}{2(m+h)}\left(ru \pm \sqrt{r^2u^2 - 4v(m+h)}\right).$$

Clearly $N_\pm \geq 0$ and $\Psi(N)$ is nonnegative in $[N_-, N_+]$, with $0 < N_- < N_* < N_+$.

Study of the curve Θ

The function $\Theta(N)$ has a vertical asymptote on the coordinate axis $N = 0$ and is positive for $0 < N < N_0$, where $N_0 = \frac{k}{\ell}$.

We also find

$$\frac{d\Theta}{dN} = u\frac{N^2 - v}{u^2N^2}(k - \ell N) - \ell\frac{v+N^2}{uN}.$$

Therefore, it is not immediately clear whether the function is monotonically decreasing. The positive condition of the first derivative is equivalent to the cubic inequality

$$-2\ell N^3 + kN^2 - vk > 0,$$

so that by the Descartes rule there are two positive roots. The question is whether they are located in the interval $[0, N_0]$. In case they are not, in the very same interval $\Theta(N)$ is monotonically decreasing and no multiple intersections with the other function arising from the equilibrium equation of N would be possible. Conversely, Θ exhibits a kink in the feasible region and multiple intersections could arise.

The second derivative of the function is

$$\frac{d^2\Theta}{dN^2} = -6\ell N^2 + k.$$

It is nonnegative for $0 < N < \widehat{N}$, where $\widehat{N} = \sqrt{\frac{k}{6\ell}}$. Therefore, we find $N_0 < \widehat{N}$ for

$$6k < \ell, \tag{13}$$

ensuring the monotonicity of $\Theta(N)$ in $[0, N_0]$.

We can further investigate the condition $\Theta'(N) < 0$ in $[0, N_0]$. It is equivalent to

$$L(N) = \ell\frac{v+N^2}{uN} < \frac{N^2 - v}{uN^2}(k - \ell N) = \widetilde{R}(N) = \frac{1}{uN^2}R(N). \tag{14}$$

Now, $L(N) \geq 0$ for every $N \in [0, N_0]$. On the other hand, $R(N) \geq 0$ for $N \in [N_*, N_0]$. This means that $L(N) < \widetilde{R}(N)$ for $0 < N < \sqrt{v}$, $N > \frac{k}{\ell}$. In $N \in [N_*, N_0]$ we need to investigate the conditions for which L and $\widetilde{R}$ intersect, as they are both positive. Rewriting (14) in the simplified form

$$\ell N(v+N^2) < (N^2 - v)(k - \ell N),$$

we can finally establish the condition for the intersections of $NL(N)$ and $R(N)$ for $N \in [N_*, N_0]$. Differentiating, we find

$$\frac{dR}{dN} = -3N^2 + kN + \ell v,$$

from which the maximum is attained at the point

$$N_{**}^+ = \frac{1}{6}\left[k + \sqrt{k^2 + 12\ell v}\right]$$

and the condition that must be satisfied is

$$N_{**}^+ L(N_{**}^+) > R(N_{**}^+). \tag{15}$$

Summarizing, (15) ensures that (14) holds, which means that $\Theta(N)$ is monotonically decreasing in $[0, N_0]$.

Intersections of the curves Ψ and Θ

Assume now the monotonicity of $\Theta(N)$, that is, (13) or (15). We need to find the intersections of the curves Ψ and Θ, as these provide the assets-free equilibrium points, in the first quadrant of the N-F plane.

There are four possible situations, the first two of which do not lead to any feasible intersection, namely

$$N_0 < N_- \quad \text{and} \quad N_0 > N_+, \tag{16}$$

conditions that will therefore be disregarded. We focus instead on the following two:

$$N_- < N_0 < N_+, \tag{17}$$

$$N_* < N_+ < N_0. \tag{18}$$

The condition (17) ensures the uniqueness of the intersection, therefore, giving an equilibrium point E_P.

On the other hand, (18) does not always ensure the existence of the intersection; in the case where Ψ and Θ are tangent to each other, uniqueness is guaranteed. Indeed, note that Ψ is concave and Θ is convex. However, if they intersect, there will be a pair of equilibria E_P through a saddle–node bifurcation. For this to occur, we need also $\Psi(N_*) < \Theta(N_*)$, which using (11) can explicitly be written as

$$2\frac{v}{u}(k - \ell\sqrt{v}) < \frac{ru}{2c} - \sqrt{v}\frac{m+h}{c}. \tag{19}$$

Feasibility of coexistence, E_*

The second equilibrium equation, that is, the equilibrium equation for F, gives the function $F = \Psi(N)$, with (10), already investigated for the assets-free equilibrium, E_P. However, the difference is that in the previous subsection this was a curve in the $N - F$ plane, while here, in the three-dimensional space, it is a cylinder with the axis parallel to the A axis.

Then, from the first equilibrium equation, i.e., the equilibrium equation for A, solving for F, we find the surface

$$F = \chi(A) = \frac{q}{bA^2}(p + A^2). \tag{20}$$

Finally, from the last equilibrium equation for N we get another surface, namely

$$F = \Phi(N, A) = \frac{(k - \ell N)(v + N^2)(z + A)}{uN(z + A) - gA(v + N^2)}. \tag{21}$$

In this case, for the coexistence feasibility, we can look for sufficient conditions to have at least one intersection point of these three surfaces, Ψ, χ, and Φ, in the first octant of the A-N-F space.

Study of the surface χ

The function $\chi(A)$, being independent of N, represents a cylinder with the axis parallel to the N axis. Its intersection with the $N = 0$ coordinate plane is a hyperbola-like function, with a vertical asymptote on the F axis and a horizontal one located at

$$F_\infty = \frac{q}{b}. \tag{22}$$

This function is monotonically decreasing in view of the fact that

$$\frac{d\chi}{dA} = -\frac{2}{bA^2} < 0.$$

Study of the surface Φ

Let us define the following quantity, the denominator of (21)

$$D_\Phi = uzN + uNA - gvA - gAN^2 = -N_\mathcal{F}(N) - AD_\mathcal{F}(N),$$

where

$$N_\mathcal{F}(N) = uzN \quad \text{and} \quad D_\mathcal{F}(N) = gN^2 - uN + gv.$$

To assess the regions for which Φ is feasible, we need to study the sign of its denominator, D_Φ, since its numerator, N_Φ, is easily seen to be positive for

$$N < N_0. \tag{23}$$

Now, $D_\Phi > 0$ is equivalent to $AD_\mathcal{F} < N_\mathcal{F}$. This inequality holds trivially for $D_\mathcal{F} < 0$. Conversely, for $D_\mathcal{F} > 0$ it reduces to

$$A \le \mathcal{F}(N) = \frac{N_\mathcal{F}}{D_\mathcal{F}}.$$

The roots of $D_\mathcal{F} = 0$ are

$$N_{u,\ell} = \frac{1}{2g}\left[u \pm \sqrt{u^2 - 4g^2v}\right],$$

where the subscript ℓ (lower) corresponding to the minus sign and u (upper) to the plus sign. Thus, in this case $D_\mathcal{F} > 0$ for $N < N_\ell$ and $N > N_u$. Combining these results, we find $D_\Phi > 0$ for the following alternative cases:

$$D_\mathcal{F} > 0 : A \le \mathcal{F}; \qquad D_\mathcal{F} > 0 : \text{always true.} \tag{24}$$

The function $A = \mathcal{F}$ has two branches in the first quadrant. The left one crosses the origin and raises up to a vertical asymptote located at $N = N_\ell$. In (N_ℓ, N_u), the function is negative, while it decreases from another vertical asymptote at $N = N_u$ to approach the horizontal axis for $N \to +\infty$.

We now concentrate on the feasibility of the function $\Phi(N, A)$. On $A = \mathcal{F}$, the surface Φ has a vertical asymptote. On the other hand, on $N = N_0$ it vanishes. The above two lines, $A = \mathcal{F}$ and $N = N_0$, intersect at the point

$$A_0 = \mathcal{F}(N_0) = \frac{\ell kuz}{g\ell^2 v - k\ell u + gk^2}, \tag{25}$$

feasible if

$$g\ell^2 v + gk^2 > k\ell.$$

Note that at the point A_0 the surface Φ does not have a limit, because if the point is approached along the curve $\mathcal{F}$, the surface grows without limit, while if A_0 is approached along the line $N = N_0$ the surface vanishes.

We have to distinguish between two different alternative situations leading to $\Phi(N, A) > 0$:

$$N_\Phi > 0, \quad D_\Phi > 0 \tag{26}$$

or

$$N_\Phi < 0, \quad D_\Phi < 0. \tag{27}$$

In the case (26), we need $N < N_0$, with no other conditions, if $D_\mathcal{F} < 0$. Instead, we need $N < N_0$ and $A \le \mathcal{F}(N)$ for $D_\mathcal{F} > 0$, compare (23) and (24). Geometrically, the latter means that the feasible region in the N-A plane lies below the two positive branches of $A = \mathcal{F}(N)$ and includes also the half stripe in the first quadrant bounded below by the interval (N_ℓ, N_u). We must further distinguish three subcases depending on the location of N_0 with respect to (N_ℓ, N_u):

(a1) $N_0 < N_\ell < N_u$: the surface Φ is positive in the "triangular" region Ω_{a1}, with a vertex at the point (N_0, A_0), bounded above by the left branch of $\mathcal{F}$, on the right by the vertical line $N = N_0$ and below by the coordinate axis N;

(a2) $N_\ell < N_0 < N_u$: the surface Φ is positive in the region Ω_{a2} bounded below by the coordinate axis N and above by the left branch of $\mathcal{F}$ for $N < N_\ell$, and in the half-stripe for $N_\ell < N < N_0$;

(a3) $N_\ell < N_u < N_0$: the surface Φ is positive in the region Ω_{a3} bounded below by the coordinate axis N, bounded above by the left branch of $\mathcal{F}$ for $N < N_\ell$, in the half-stripe for $N_\ell < N < N_u$ and bounded above by the right branch of $\mathcal{F}$ for $N_u < N < N_0$.

In the case (27), we need $N > N_0$ and $A > \mathcal{F}(N)$ for $D_\mathcal{F} > 0$; the condition does not hold if $D_\mathcal{F} < 0$. Hence, $\Phi(N, A)$ is positive only above the function $\mathcal{F}$ whenever this is positive. Here, too, there are three subcases:

(b1) $N_0 < N_\ell < N_u$: the surface Φ is positive in the region Ω_{b1} above the left branch of $\mathcal{F}$ for $N_0 < N < N_\ell$ and above the right branch of $\mathcal{F}$ for $N > N_u$;

(b2) $N_\ell < N_0 < N_u$: the surface Φ is positive in the region Ω_{b2} above the right branch of $\mathcal{F}$, i.e., for $N > N_u$;

(b3) $N_\ell < N_u < N_0$: the surface Φ is positive in the region Ω_{b3} above the right branch of $\mathcal{F}$ for $N > N_0$.

Note also that the surface Φ in the regions that are unbounded has different behaviors, namely

$$\lim_{N \to +\infty} \Phi(N, A) = +\infty,$$

Table 6
Intersections of $\widetilde{\Lambda}$ with Φ in the case (a1).

Intersections	Conditions
No intersection	if $N_0 < N_-^\infty$
Unique intersection	• for $N_-^\infty < N_0 < N_*$, iff $\Lambda(N_0) < A_0$ • for $N_* < N_0 < N_\ell < N_+^\infty$, iff $\Lambda(N_0) < A_0$
Two intersections	for $N_* < N_+^\infty < N_0 < N_\ell$, if $\widetilde{\Lambda}(N_*, A_X) > \Phi(N_*, A_X)$

Table 7
Intersections of $\widetilde{\Lambda}$ with Φ in the case (a2).

Intersections	Conditions
No intersection	• if $N_0 < N_-^\infty$ • for $N_+^\infty < N_\ell$, if $\widetilde{\Lambda}(N_*, A_X) > \Phi(N_*, A_X)$
Unique intersection in $[N_-^\infty, N_0]$	• for $N_\ell < N_-^\infty < N_0 < N_+^\infty$, if not (28) • for $N_-^\infty < N_\ell < N_0 < N_+^\infty$
Two intersections in $[N_-^\infty, N_+^\infty]$	• for $N_\ell < N_-^\infty < N_+^\infty < N_0$ – if $\widetilde{\Lambda}(N_*, A_X) > \Phi(N_*, A_X)$ and not (28) – if $\widetilde{\Lambda}(N_*, A_X) < \Phi(N_*, A_X)$ and (28) • for $N_+^\infty < N_\ell$, if $\widetilde{\Lambda}(N_*, A_X) < \Phi(N_*, A_X)$ • for $N_-^\infty < N_\ell < N_+^\infty < N_0$ – if $\widetilde{\Lambda}(N_*, A_X) > \Phi(N_*, A_X)$ and not (28) – if $\widetilde{\Lambda}(N_*, A_X) < \Phi(N_*, A_X)$ and (28)

Table 8
Intersections of $\widetilde{\Lambda}$ with Φ in the case (a3).

Intersections	Conditions
No intersection	• if $N_0 < N_-^\infty$ • for $N_u < N_-^\infty < N_0 < N_+^\infty$, if $\Lambda(N_0) > \mathcal{F}(N_0)$ • for $N_\ell < N_-^\infty < N_u < N_0 < N_+^\infty$, if $\Lambda(N_0) < \mathcal{F}(N_0)$ • for $N_u < N_-^\infty < N_+^\infty < N_0$, if $\Lambda(N_*) > \mathcal{F}(N_*)$ • for $N_-^\infty < N_+^\infty < N_\ell < N_u < N_0$, if $\Lambda(N_X) > \mathcal{F}(N_X)$
Unique intersection in $[N_-^\infty, N_0]$	• for $N_u < N_-^\infty < N_0 < N_+^\infty$, if $\Lambda(N_0) < \mathcal{F}(N_0)$ • for $N_\ell < N_-^\infty < N_u < N_0 < N_+^\infty$, if $\Lambda(N_0) > \mathcal{F}(N_0)$
Unique intersection in $[N_-^\infty, N_u]$	for $N_-^\infty < N_\ell < N_u < N_0 < N_+^\infty$, if $\Lambda(N_0) < \mathcal{F}(N_0)$
Two intersections in $[N_-^\infty, N_+^\infty]$	• for $N_-^\infty < N_+^\infty < N_\ell < N_u < N_0$, if $\Lambda(N_X) < \mathcal{F}(N_X)$ • for $N_\ell < N_-^\infty < N_+^\infty < N_u < N_0$ – if $\widetilde{\Lambda}(N_X, A_X) < \Phi(N_X, A_X)$ and not (28) – if $\widetilde{\Lambda}(N_X, A_X) > \Phi(N_X, A_X)$ and (28) • for $N_\ell < N_-^\infty < N_u < N_+^\infty < N_0$ – if $\widetilde{\Lambda}(N_X, A_X) < \Phi(N_X, A_X)$ and not (28) – if $\widetilde{\Lambda}(N_X, A_X) > \Phi(N_X, A_X)$ and (28) • for $N_u < N_-^\infty < N_+^\infty < N_0$, if $\Lambda(N_*) < \mathcal{F}(N_*)$ • for $N_-^\infty < N_\ell < N_u < N_+^\infty < N_0$ • for $N_-^\infty < N_\ell < N_u < N_0 < N_+^\infty$, if $\Lambda(N_0) > \mathcal{F}(N_0)$ • for $N_-^\infty < N_\ell < N_+^\infty < N_u < N_0$ – if $\widetilde{\Lambda}(N_X, A_X) < \Phi(N_X, A_X)$ and not (28) – if $\widetilde{\Lambda}(N_X, A_X) > \Phi(N_X, A_X)$ and (28)

while

$$\lim_{A\to+\infty} \Phi(N, A) = \frac{(k - \ell N)(v + N^2)}{uN - g(v + N^2)},$$

whose value depends on N but it is finite.

Study of the curve $\widetilde{\Lambda} = \chi \cap \Psi$

In the following analysis, some cases will hinge on the mutual behavior of Φ and $\widetilde{\Lambda} = \chi \cap \Psi$ as $a \to +\infty$. The latter is above the surface if the following inequality holds, and conversely:

$$\frac{(k - \ell N)(v + N^2)}{uN - g(v + N^2)} < \frac{q}{b}. \tag{28}$$

We now turn to studying the curve $\widetilde{\Lambda} = \chi \cap \Psi$. Because the former is above the plane $F = qb^{-1}$ and the latter has the height of the maximum $F = \Psi(N_*, \widehat{A})$, $\widehat{A}$ being an arbitrary value as Ψ is a cylinder, they can intersect only if $\Psi(N_*, \widehat{A}) > qb^{-1}$, a condition that explicitly becomes

$$bru > 2cqv + 2b(m + h)v. \tag{29}$$

Because χ raises up to infinity for $A = 0$, i.e., on the N-F coordinate plane, for increasing A it decreases toward its horizontal asymptote. The first intersection with the cylinder Ψ must occur at a point $X = (A_X, F_X, N_X)$, with $N_X = N_* = \sqrt{v} > 0$. We must then have $\chi(N_*, A_X) = \Psi(N_*, A_X)$, from which follows

$$A_X = \sqrt{\frac{2cpqv}{bru - 2cqv - 2bv(m + h)}}.$$

The intersection exists only if $A_X \geq 0$, that is, if (29) holds. Finally, we explicitly have

$$X = (A_X, \Psi(\sqrt{v}), \sqrt{v}).$$

The curve $\widetilde{\Lambda} = \chi \cap \Psi$ originates from X and consists of two branches, $\widetilde{\Lambda}_-$ and $\widetilde{\Lambda}_+$, respectively, for $N \leq N_*$ and $N \geq N_*$. In view of the fact that they lie on χ, as $A \to +\infty$ both approach $F = qb^{-1}$ and on this plane also, respectively, approach the values $N = N_{\mp}^\infty$, with $N_- < N_-^\infty$ and $N_+^\infty < N_+$. The latter is obtained by imposing that $\Psi(N) = qb^{-1}$. We find

$$N_{\mp}^\infty = \frac{1}{2[cq + b(m + h)]} \left[bru \pm \sqrt{b^2r^2u^2 - 4[cq + b(m + h)]^2 v} \right].$$

Table 9
Intersections of $\widetilde{\Lambda}$ with Φ in the case (b1).

Intersections	Conditions
No intersection	• for $N_-^\infty < N_+^\infty < N_0 < N_\ell < N_u$ • for $N_-^\infty < N_0 < N_\ell < N_+^\infty < N_u$, if $\Lambda(N_X) < \mathcal{F}(N_X)$ • for $N_-^\infty < N_0 < N_\ell < N_u < N_+^\infty$, if $\Lambda(N_X) < \mathcal{F}(N_X)$ and not (28) • for $N_0 < N_-^\infty < N_+^\infty < N_\ell < N_u$, if not (28) and $\widetilde{\Lambda}(N_X, A_X) < \Phi(N_X, A_X)$ • for $N_0 < N_\ell < N_-^\infty < N_+^\infty < N_u$ • for $N_0 < N_\ell < N_u < N_-^\infty < N_+^\infty$, if not (28)
One intersection	• for $N_-^\infty < N_0 < N_+^\infty < N_\ell < N_u$, if not (28) • for $N_-^\infty < N_0 < N_\ell < N_+^\infty < N_u$, if $\Lambda(N_X) > \mathcal{F}(N_X)$ • for $N_-^\infty < N_0 < N_\ell < N_u < N_+^\infty$ – if $\Lambda(N_X) > \mathcal{F}(N_X)$ and not (28) – if $\Lambda(N_X) < \mathcal{F}(N_X)$ and (28)
One intersection in $[N_-^\infty, N_\ell]$	• for $N_0 < N_-^\infty < N_\ell < N_+^\infty < N_u$ • for $N_0 < N_-^\infty < N_\ell < N_u < N_+^\infty$
One intersection in $[N_u, N_+^\infty]$	for $N_0 < N_\ell < N_-^\infty < N_u < N_+^\infty$, if (28)
Two intersections	• for $N_-^\infty < N_0 < N_\ell < N_u < N_+^\infty$, if $\Lambda(N_X) > \mathcal{F}(N_X)$ and (28) • for $N_0 < N_-^\infty < N_+^\infty < N_\ell < N_u$, if (28) and $\widetilde{\Lambda}(N_X, A_X) < \Phi(N_X, A_X)$ • for $N_0 < N_-^\infty < N_+^\infty < N_\ell < N_u$ – if $\Lambda(N_X) < \mathcal{F}(N_X)$ and (28) – if $\Lambda(N_X) > \mathcal{F}(N_X)$ and not (28) • for $N_0 < N_\ell < N_u < N_-^\infty < N_+^\infty$, if $\Lambda(N_X) < \mathcal{F}(N_X)$ and (28) • for $N_0 < N_-^\infty < N_\ell < N_u < N_+^\infty$, if (28)

Table 10
Intersections of $\widetilde{\Lambda}$ with Φ in the case (b2).

Intersections	Conditions
No intersection	• for $N_-^\infty < N_+^\infty < N_\ell < N_u$ – if $\Lambda(N_X) > \mathcal{F}(N_X)$ and (28) – if $\Lambda(N_X) < \mathcal{F}(N_X)$ and not (28) • for $N_-^\infty < N_\ell < N_u < N_+^\infty$, if not (28) • for $N_\ell < N_-^\infty < N_+^\infty < N_u$ • for $N_\ell < N_-^\infty < N_u < N_+^\infty$, if not (28) • for $N_\ell < N_u < N_-^\infty < N_+^\infty$ – if $\Lambda(N_X) > \mathcal{F}(N_X)$ and (28) – if $\Lambda(N_X) < \mathcal{F}(N_X)$ and not (28)
One intersection	• for $N_-^\infty < N_+^\infty < N_\ell < N_u$, if (28) • for $N_\ell < N_-^\infty < N_u < N_+^\infty$, if (28)
Two intersections	• for $N_-^\infty < N_+^\infty < N_\ell < N_u$, if $\Lambda(N_X) > \mathcal{F}(N_X)$ and (28) • for $N_-^\infty < N_\ell < N_+^\infty < N_u$, if (28) • for $N_-^\infty < N_\ell < N_u < N_+^\infty$, if (28) • for $N_\ell < N_u < N_-^\infty < N_+^\infty$ – if $\Lambda(N_X) > \mathcal{F}(N_X)$ and not (28) – if $\Lambda(N_X) < \mathcal{F}(N_X)$ and (28)

Intersections of the curve $\widetilde{\Lambda}$ with the surface Φ

Coexistence is obtained from the intersection of the curve $\widetilde{\Lambda}$ with the surface Φ. Several situations can arise, due to the various cases (a1)–(a3) and (b1)–(b3) examined above, in combination with the location of the point X, the branches of $\widetilde{\Lambda}$, and their asymptotes at $N_\mp^\infty$. The existence of the intersection relies on the fact that in the phase space the curve $\widetilde{\Lambda}$ approaches the horizontal plane $F = F_\infty$, see (22), and that on $\mathcal{F}(N)$ the function Φ has a vertical asymptote.

Our discussion focuses mainly on the location of the projection of the point X, (N_X, A_X) on the N-A coordinate plane, from which the projection $A = \Lambda(N)$ of the curve $\widetilde{\Lambda}$ originates, and the feasible regions where $\Phi \geq 0$ discovered in (a1)–(a3) and (b1)–(b3) above. Note that the curve Λ has vertical asymptotes at $N = N_\mp^\infty$.

The cases that can arise are many, too many to list exhaustively. In addition, in several of them it is not clear whether the intersection is unique or, in some cases, multiple (in general, double). In the latter case, there would most likely be saddle–node bifurcations giving rise to pairs of equilibria, but to specify the conditions under which they arise would be very difficult, also because the coordinates of the coexistence equilibrium point are not explicit. We therefore confine ourselves to list the cases where the existence and uniqueness of the coexistence equilibrium occur and disregard other more complicated situations. See Tables 6, 7, 8, 9, 10, and 11.

Data availability

No data was used for the research described in the article.

Table 11
Intersections of $\widetilde{\Lambda}$ with Φ in the case (b3).

Intersections	Conditions
No intersection	• for $N_-^\infty < N_+^\infty < N_\ell < N_u < N_0$ • for $N_-^\infty < N_\ell < N_+^\infty < N_u < N_0$ • for $N_-^\infty < N_\ell < N_u < N_+^\infty < N_0$ • for $N_\ell < N_-^\infty < N_+^\infty < N_u < N_0$ • for $N_\ell < N_-^\infty < N_u < N_+^\infty < N_0$ • for $N_\ell < N_u < N_-^\infty < N_+^\infty < N_0$, if $\Lambda(N_X) > \mathcal{F}(N_X)$ • for $N_\ell < N_u < N_-^\infty < N_0 < N_+^\infty$, if $\widetilde{\Lambda}(N_X, A_X) < \Phi(N_X, A_X)$ • for $N_\ell < N_u < N_0 < N_-^\infty < N_+^\infty$ if $\Lambda(N_X) > \mathcal{F}(N_X)$ – if $\widetilde{\Lambda}(N_X, A_X) > \Phi(N_X, A_X)$ and (28) – if $\widetilde{\Lambda}(N_X, A_X) < \Phi(N_X, A_X)$ and not (28)
One intersection	• for $N_-^\infty < N_\ell < N_u < N_0 < N_+^\infty$, if (28) • for $N_\ell < N_-^\infty < N_u < N_0 < N_+^\infty$, if (28) • for $N_\ell < N_u < N_-^\infty < N_0 < N_+^\infty$, if $\widetilde{\Lambda}(N_X, A_X) > \Phi(N_X, A_X)$ and $\Lambda(N_0) > \mathcal{F}(N_0)$ or $\Lambda(N_0) < \mathcal{F}(N_0)$
Two intersections	• for $N_\ell < N_u < N_-^\infty < N_+^\infty < N_0$, if $\Lambda(N_X) < \mathcal{F}(N_X)$ • for $N_\ell < N_u < N_0 < N_-^\infty < N_+^\infty$, if $\Lambda(N_X) < \mathcal{F}(N_X)$ – if $\widetilde{\Lambda}(N_X, A_X) > \Phi(N_X, A_X)$ and not (28) – if $\widetilde{\Lambda}(N_X, A_X) < \Phi(N_X, A_X)$ and (28)

References

Abdul Latif Jameel Poverty Action Lab (J-PAL), 2019. Facilitating Savings Among Smallholder Farmers to Smooth or Increase Consumption. J-PAL Policy Insights, URL https://doi.org/10.31485/pi.2417.2019. Last modified May 2019.

Alkire, S., Conconi, A., Robles, G., Seth, S., 2015. Multidimensional poverty index, winter 2014/2015: brief methodological note and results. OPHI Brief. 27, 1–3.

Asamoah, E.K., Ewusie Nunoo, F.K., Osei-Asare, Y.B., Addo, S., Sumaila, U.R., 2012. A production function analysis of pond aquaculture in Southern Ghana. Aquac. Econ. Manag. 16 (3), 183–201.

Banitz, T., Schlüter, M., Lindkvist, E., Radosavljevic, S., Johansson, L.G., Ylikoski, P., Martínez-Peña, R., Grimm, V., 2022. Model-derived causal explanations are inherently constrained by hidden assumptions and context: The example of baltic cod dynamics. Environ. Model. Softw. 156, 105489.

Barrett, C.B., Carter, M.R., 2013. The economics of poverty traps and persistent poverty: empirical and policy implications. J. Dev. Stud. 49 (7), 976–990.

Barrett, C.B., Garg, T., McBride, L., 2016. Well-being dynamics and poverty traps. Annu. Rev. Resour. Econ. 8 (1), 303–327.

Barro, R., Sala-i Martin, X., 2004. Economic Growth, second ed. MIT Press, t. Cambridge, Massachusetts.

Belton, B., 2013. Small-Scale Aquaculture, Development and Poverty: a Reassessment. FAO.

Belton, B., Little, D.C., 2011. Immanent and interventionist inland Asian aquaculture development and its outcomes. Dev. Policy Rev. 29 (4), 459–484.

Béné, C., Arthur, R., Norbury, H., Allison, E.H., Beveridge, M., Bush, S., others, Williams, M., 2016. Contribution of fisheries and aquaculture to food security and poverty reduction: assessing the current evidence. World Dev. 79, 177–196.

Bialozyt, R.B., Roß-Nickoll, M., Ottermanns, R., Jetzkowitz, J., 2025. The different ways to operationalise the social in applied models and simulations of sustainability science: A contribution for the enhancement of good modelling practices. Ecol. Model. 500, 110952.

Bieg, C., Vasseur, D., 2024. Interactions between temperature and nutrients determine the population dynamics of primary producers. Ecol. Lett. 27 (1), e14363.

Blume, L.E., Durlauf, S.N., Lukina, A., 2020. Poverty traps in Markov models of the evolution of wealth. In: WZB Discussion Paper. Wissenschaftszentrum Berlin Für Sozialforschung (WZB), Berlin.

Boughton, D., Goeb, J., Lambrecht, I., Headey, D., Takeshima, H., Mahrt, K., others, Diao, X., 2021. Impacts of COVID-19 on agricultural production and food systems in late transforming southeast Asia: The case of Myanmar. Agricult. Sys. 188, 103026.

Boyd, C.E., Tucker, C.S., Boyd, C.E., Tucker, C.S., 1998. Ecology of aquaculture ponds. In: Pond Aquaculture Water Quality Management. Springer US, Boston, MA, pp. 8–86.

Clark, C.W., 2010. Mathematical Bioeconomics: the Mathematics of Conservation, vol. 91, John Wiley & Sons.

Cramb, R., Purcell, T., Ho, T., 2004. Participatory assessment of rural livelihoods in the central highlands of Vietnam. Agricult. Sys. 81 (3), 255–272.

Dam Lam, R., Barman, B.K., Lozano Lazo, D.P., Khatun, Z., Parvin, L., Choudhury, A., others, Gasparatos, A., 2022. Sustainability impacts of ecosystem approaches to small-scale aquaculture in Bangladesh. Sustain. Sci. 17 (1), 295–313.

De Silva, S.S., Davy, F.B., 2010. Success Stories in Asian Aquaculture. IDRC, Ottawa, ON, CA.

Dompreh, E.B., Rossignoli, C.M., Griffiths, D., Wang, Q., Htoo, K.K., Nway, H.M., others, Gasparatos, A., 2024. Impact of adoption of better management practices and nutrition-sensitive training on the productivity, livelihoods and food security of small-scale aquaculture producers in Myanmar. Food Secur. 16 (3), 757–780.

Eppinga, M.B., Reader, M.O., Santos, M.J., 2024. Exploratory modeling of social-ecological systems. Ecosphere 15 (10), e70037.

FAO, 2020. The state of food and agriculture 2020.

Filipski, M., Belton, B., 2018. Give a man a fishpond: modeling the impacts of aquaculture in the rural economy. World Dev. 110, 205–223.

Fish for Livelihoods, 2022. Annual progress report 1.10.2021-30.9.2022. URL https://mel.cgiar.org/projects/1211.

Gephart, J.A., Henriksson, P.J., Parker, R.W., Shepon, A., Gorospe, K.D., Bergman, K., Eshel, G., Golden, C.D., Halpern, B.S., Hornborg, S., et al., 2021. Environmental performance of blue foods. Nature 597 (7876), 360–365.

Haider, L.J., Boonstra, W.J., Peterson, G.D., Schlüter, M., 2018. Traps and sustainable development in rural areas: A review. World Dev. 101, 311–321.

Henriksson, P.J.G., Troell, M., Banks, L.K., Belton, B., Beveridge, M.C.M., Klinger, D.H., Pelletier, N., Phillips, M.J., Tran, N., 2021. Interventions for improving the productivity and environmental performance of global aquaculture for future food security. One Earth 4 (9), 1220–1232.

Hoover, C.M., Sokolow, S.H., Kemp, J., Sanchirico, J.N., Lund, A.J., Jones, I.J., others, De Leo, G.A., 2019. Modelled effects of prawn aquaculture on poverty alleviation and schistosomiasis control. Nat. Sustain. 2 (7), 611–620.

Jakeman, A.J., Elsawah, S., Wang, H.-H., Hamilton, S.H., Melsen, L., Grimm, V., 2024. Towards normalizing good practice across the whole modeling cycle: its instrumentation and future research topics. Socio Environ. Syst. Model. 6, 18755.

Jobling, M., 2003. The thermal growth coefficient model of fish growth: a cautionary note. Aquacult. Res. 34, 581–584.

Kang, Y., Baidya, A., Aaron, A., Wang, J., Chan, C., Wetzler, E., 2021. Differences in the early impact of COVID-19 on food security and livelihoods in rural and urban areas in the Asia Pacific region. Glob. Food Secur. 31, 100580.

Kooijman, S.A.L.M., 2010. Dynamic Energy Budget Theory for Metabolic Organisation. Cambridge University Press, Great Britain.

Kraay, A., Raddatz, C., 2007. Poverty traps, aid, and growth. J. Dev. Econ. 82 (2), 315–347.

Kvamsdal, S.F., Maroto, J.M., Morán, M., Sandal, L.K., 2020. Bioeconomic modeling of seasonal fisheries. European J. Oper. Res. 281 (2), 332–340.

Lade, S.J., Haider, L.J., Engström, G., Schlüter, M., 2017. Resilience offers escape from trapped thinking on poverty alleviation. Sci. Adv. 3 (5), e1603043.

Levin, S., Xepapadeas, T., Crépin, A.S., Norberg, J., De Zeeuw, A., Folke, C., Hughes, T., Arrow, K., Barrett, S., Daily, G., et al., 2013. Social-ecological systems as complex adaptive systems: modeling and policy implications. Environ. Dev. Econ. 18 (2), 111–132.

Little, D.C., Young, J.A., Zhang, W., Newton, R.W., Al Mamun, A., Murray, F.J., 2018. Sustainable intensification of aquaculture value chains between Asia and Europe: A framework for understanding impacts and challenges. Aquaculture 493, 338–354.

Lu, Z., 2003. Modeling of Water Temperature, Dissolved Oxygen, and Fish Growth Rate in Stratified Fish Ponds Using Stochastic Input Variables (Ph.D. thesis). University of California, Davis.

Luna, M., Llorente, I., Luna, L., 2023. A conceptual framework for risk management in aquaculture. Mar. Policy 147, 105377.

Milstein, A., 1992. Ecological aspects of fish species interactions in polyculture ponds. Hydrobiologia 231 (3), 177–186.

Mitra, S., Khan, M.A., Nielsen, R., 2019. Credit constraints and aquaculture productivity. Aquac. Econ. Manag. 23 (4), 410–427.

Nagel, B., Buhari, N., Partelow, S., 2024. Archetypes of community-based pond aquaculture in Indonesia: applying the social-ecological systems framework to examine sustainability tradeoffs. Environ. Res. Lett. 19 (4), 044026.

Naylor, R., Fang, S., Fanzo, J., 2023. A global view of aquaculture policy. Food Policy 116, 102422.

Naylor, R., Hardy, R., Buschmann, A., Bush, S., Cao, L., Klinger, D., Little, D., Lubchenco, J., Shumway, S., Troell, M., 2021. A 20-year retrospective review of global aquaculture. Nature 591 (7851), 551–563.

Ngonghala, C.N., De Leo, G.A., Pascual, M.M., Keenan, D.C., Dobson, A.P., Bonds, M.H., 2017. General ecological models for human subsistence, health and poverty. Nat. Ecol. Evol. 1 (8), 1153–1159.

Ngonghala, C.N., Pluciński, M.M., Murray, M.B., Farmer, P.E., Barrett, C.B., Keenan, D.C., Bonds, M.H., 2014. Poverty, disease, and the ecology of complex systems. PLoS Biol. 12 (4), e1001827.

Nobre, A.M., Musango, J.K., De Wit, M.P., Ferreira, J.G., 2009. A dynamic ecological–economic modeling approach for aquaculture management. Ecol. Econom. 68 (12), 3007–3017.

Nugroho, S., 2025. Operationalizing social-ecological system-based fishery management employing a system dynamics model: Lessons from eel fishery. Ecol. Model. 509, 111276.

Pant, J., Barman, B.K., Murshed-E-Jahan, K., Belton, B., Beveridge, M., 2014. Can aquaculture benefit the extreme poor? A case study of landless and socially marginalized adivasi (ethnic) communities in Bangladesh. Aquaculture 418, 1–10.

Partelow, S., Schlüter, A., O. Manlosa, A., Nagel, B., Octa Paramita, A., 2022. Governing aquaculture commons. Rev. Aquac. 14 (2), 729–750.

Partelow, S., Senff, P., Buhari, N., Schlüter, A., 2018. Operationalizing the social-ecological systems framework in pond aquaculture. Int. J. Commons 12 (1), 485–518.

Radosavljevic, S., Banitz, T., Grimm, V., Johansson, L.G., Lindkvist, E., Schlüter, M., Ylikoski, P., 2023. Dynamical systems modeling for structural understanding of social-ecological systems: a primer. Ecol. Complex. 56, 101052.

Radosavljevic, S., Haider, L.J., Lade, S.J., Schlüter, M., 2020. Effective alleviation of rural poverty depends on the interplay between productivity, nutrients, water and soil quality. Ecol. Econom. 169, 106494.

Radosavljevic, S., Haider, L.J., Lade, S.J., Schlüter, M., 2021. Implications of poverty traps across levels. World Dev. 144, 105437.

Radosavljevic, S., Sanga, U., Schlüter, M., 2024. Navigating simplicity and complexity of social-ecological systems through a dialogue between dynamical systems and agent-based models. Ecol. Model. 495, 110788.

Rahman, M.T., Nielsen, R., Khan, M.A., Ahsan, D., 2021. Perceived risk and risk management strategies in pond aquaculture. Mar. Resour. Econ. 36 (1), 43–69.

Rossignoli, C.M., Lozano Lazo, D.P., Barman, B.K., Dompreh, E.B., Manyise, T., Wang, Q., others, Gasparatos, A., 2023a. Multi-stakeholder perception analysis of the status, characteristics, and factors affecting small-scale carp aquaculture systems in Bangladesh. Front. Sustain. Food Syst. 7, 1121434.

Rossignoli, C.M., Manyise, T., Shikuku, K.M., Nasr-Allah, A.M., Dompreh, E.B., Henriksson, P.J., others, Gasparatos, A., 2023b. Tilapia aquaculture systems in Egypt: Characteristics, sustainability outcomes and entry points for sustainable aquatic food systems. Aquaculture 577, 739952.

Sanga, U., Radosavljevic, S., Schluter, M., 2024. Emergence of cross-level poverty traps in agricultural innovations systems: Environmental impacts and sustainable interventions. http://dx.doi.org/10.17605/OSF.IO/HZ8TU, Available At SSRN 5290453.

Scheffer, M., 1989. Alternative stable states in eutrophic, shallow freshwater systems: a minimal model. Hydrobiol. Bull. 23, 73–83.

Schlüter, M., Hertz, T., Mancilla García, M., Banitz, T., Grimm, V., Johansson, L.-G., Lindkvist, E., Martínez-Peña, R., Radosavljevic, S., Wennberg, K., et al., 2024. Navigating causal reasoning in sustainability science. Ambio 53 (11), 1618–1631.

Svirezhev, Y.M., Krysanova, V.P., Voinov, A.A., 1984. Mathematical modelling of a fishpond ecosystem. Ecol. Model. 21 (4), 315–337.

Varga, M., Berzi-Nagy, L., Csukas, B., Gyalog, G., 2020. Long-term dynamic simulation of environmental impacts on ecosystem-based pond aquaculture. Environ. Model. Softw. 134, 104755.

Wang, Q., Rossignoli, C.M., Dompreh, E.B., Su, J., Ali, S.A., Karim, M., Gasparatos, A., 2023. Sustainable intensification of small-scale aquaculture production in Myanmar through diversification and better management practices. Environ. Res. Lett. 18 (1), 015002.

Wang, Q., Rossignoli, C.M., Dompreh, E.B., Su, J., Griffiths, D., Htoo, K.K., Nway, H.M., Akester, M., Gasparatos, A., 2024. Diversification strategies have a stabilizing effect for income and food availability during livelihood shocks: Evidence from small-scale aquaculture-agriculture systems in Myanmar during the COVID-19 pandemic. Agricult. Sys. 217, 103935.